DEVELOPMENT OF ZIF-8 BASED MIXED MATRIX MEMBRANES FOR OXYGEN ENRICHED AIR APPLICATIONS

BY

AMERUDDIN MOHAMMED KHAJA

A Thesis Presented to the
DEANSHIP OF GRADUATE STUDIES

KING FAHD UNIVERSITY OF PETROLEUM & MINERALS

DHAHRAN, SAUDI ARABIA

In Partial Fulfillment of the
Requirements for the Degree of

MASTER OF SCIENCE

In

MATERIALS SCIENCE ENGINEERING

MAY 2017

KING FAHD UNIVERSITY OF PETROLEUM & MINERALS

DHAHRAN- 31261, SAUDI ARABIA

DEANSHIP OF GRADUATE STUDIES

This thesis, written by **AMERUDDIN MOHAMMED KHAJA** under the direction his thesis advisor and approved by his thesis committee, has been presented and accepted by the Dean of Graduate Studies, in partial fulfillment of the requirements for the degree of **MASTER OF SCIENCE IN MATERIALS SCIENCE & ENGINEERING.**

Dr. Khaled Mezghani
(Advisor)

Dr. Zuhair M. A. Gasem
Department Chairman

Dr. Abdul Samad Mohammed
(Member)

Dr. Salam A. Zummo
Dean of Graduate Studies

Dr. Ahmed A. Sorour
(Member)

15/11/17

Date

Dedication

I dedicate this work to my parents, especially my father who has always supported me and encouraged me to pursue Master's degree.

ACKNOWLEDGMENTS

All praise and thanks are due to almighty Allah alone for his guidance throughout my M.Sc. Thesis program.

I acknowledge King Fahd University of Petroleum & Minerals (KFUPM) for giving me an opportunity to pursue my Master's Degree with the scholarship program.

I really appreciate and acknowledge the continuous effort and guidance of my Thesis advisor, Dr. Khaled Mezghani in my research work. Apart from his will to bring out more quality to the research work, he also made sure that all the materials and equipment are available to carry out my Thesis work smoothly. I sincerely thank him and am grateful to have him as an advisor.

I would also like to thank my Thesis committee members, Dr. Abdul Samad Mohammed and Dr. Ahmad A. Sorour for their effort to assist and evaluate my research. I would like to thank the organization KACST-TIC for their funding. Moreover, I would also like to thank Mr. Sarfaraz Ahmed, Mr. Tanveerulla Hussain and Mr. Ameer Hamza for their assistance in my research. I also thank Lab engineers, Mr. Abdul Latif and Mr. Ahmed and Mr. Abdulaziz for their help in carrying out various characterizations of my samples.

I would like to thank my roommates Shahab, Raghib and all my friends, Faisal, Allahbaksh, Ata, Basheer who made my stay at KFUPM a memorable experience. I also thank all my seniors for their support and guidance. Finally, I am grateful to my parents who patiently supported and prayed for my success throughout my journey at KFUPM.

TABLE OF CONTENTS

LIST OF TABLES

LIST OF FIGURES

LIST OF ABBREVIATIONS

2-MeIm	2-Methyl Imidazole
BET	Brunauer - Emmett - Teller
CMS	Carbon Molecular Sieves
DFT	Density Functional Theory
DSC	Differential Scanning Calorimetry
FWHM	Full Width Half Maximum
MOFs	Metal Organic Frameworks
MeOH	Methanol
MMM	Mixed Matrix Membrane
PPEES	Poly 1,4-Phenylen Ether-Ether-Sulfone
PSF	Poly Sulfone
SEM	Scanning Electron Microscopy
TGA	Thermo-Gravimetric Analysis
XRD	X-Ray Diffraction
ZIF-8	Zeolitic Imidazole Framework-8

ABSTRACT

Full Name : Ameruddin Mohammed Khaja

Thesis Title : Development of ZIF-8 based Mixed Matrix Membranes for Oxygen Enriched Air Applications

Major Field : Materials Science Engineering

Date of Degree : May, 2017

Over the past few decades membrane-based gas separation processes have been an important subject for academic research worldwide. Separation of air molecules (O_2 and N_2) to produce oxygen enriched air has been of great significance for various applications such as oxy-fuel combustion, medical respiration, etc. Mixed Matrix Membranes (MMM) containing a continuous polymer phase and a dispersed inorganic filler phase have good potential to be one of the leading materials for air separation.

In the present study, Matrimid was selected as the polymer phase in MMM because of its high selectivity, 6 to 8 for O_2/N_2 gas separation. Zeolitic Imidazolate Framework (ZIF-8) was selected as the filler phase due to its high permeability of O_2, about 400 barrers. The objective of the work was to enhance the O_2/N_2 gas separation performance of MMMs by varying the annealing temperature, time, and the ZIF-8 content in MMMs. In addition, the effect of chemical treatment on MMMs was also studied.

Pure Matrimid membranes were prepared by solution casting and annealed under vacuum at different temperatures (80 to 320°C) for various time durations (1 to 36 h). It was found that the selectivity increased significantly as the annealing temperature and time were increased. The optimum annealing temperature and time for high O_2/N_2 gas separation

were found to be 320°C and 12 hours, respectively. The permeability and selectivity at the optimum annealing temperature and time were found to be 0.36 barrers and 15.9 respectively.

Mixed Matrix Membranes were prepared by varying the amount of ZIF-8 and annealed at 320°C for 12 h. The ZIF-8 nanocrystals were synthesized at room temperature with an average crystal size of 29 nm, as determined using x-ray diffraction technique. The permeability was found to increase from 0.61 to 1.81 barrers as the loading of ZIF-8 in MMMs was increased from 5 to 40 wt%, while selectivity remained almost the same. To further enhance the O_2/N_2 gas separation performance, MMM with 43 wt% ZIF-8 was annealed at 320°C for 24 h. The permeability and selectivity was found to be 1.11 barrers and 11.86 respectively, which surpassed Robeson upper bound and falls into commercially attractive region. MMMs were also treated chemically with Ethanol and Ethylene glycol, and the results showed a decrease in O_2/N_2 gas separation performance.

ملخص الرسالة

الاسم الكامل: عامر الدين محمد خاجة

عنوان الرسالة: تطوير الأغشية المخصبة بمادة زيف-٨ لأنتاج هواء غني بالأوكسجين لتطبيقات عدة

التخصص: هندسة علوم المواد

تاريخ الدرجة العلمية: مايو، ٢٠١٧

على مدى العقود القليلة الماضية كانت عمليات فصل الغاز القائمة على الغشاء موضوعا للبحث الأكاديمي في جميع المجالات لإنتاج هواء غنيا بالأكسجين. المنتج له تطبيقات عديدة مثل احتراق الوقود مع الأوكسجين النقي، والتنفس الطبي، الخ. لهذا الغرض يمكن استعمال أغشية البوليمر المخلطة بمواد غير عضوية وذلك لخاصيتها المتفوقة على الأغشية التقليدية.

في هذه الدراسة، تم اختيار البوليمر ماتريميد لأنه يظهر انتقائية عالية لفصل غاز الأكسجين عن النتروجين بمقدار من ٦ إلى ٨ وحدات. و كذلك تم اختيار المادة الغير عضوية زيوليت إيميدازولات (زيف-٨) بسبب نفاذيتها العالية لغاز الأكسجين، حوالي ٤٠٠ بارار. الهدف من البحث هو تحسين أداء عملية فصل غاز الأكسجين عن طريق أغشية البوليمر المخلطة وذلك بتغيير كل من درجة حرارة التلدين، الزمن ومحتوى زيف-٨ الوزني داخل الأغشية المخلطة. وبالإضافة إلى ذلك، تم أيضا دراسة تأثير المعالجة الكيميائية على أداء الأغشية البوليمرية المخلطة.

تم إعداد غشاء ماتريميد عن طريق السباكة السائلة والتلدين تحت الضغط الفراغي عند درجات حرارة مختلفة (٨٠ إلى ٣٢٠ درجة مئوية) لفترات زمنية مختلفة (من ١ إلى ٣٦ ساعة). وقد وجد أن الانتقائية زادت بشكل ملحوظ مع زيادة درجة حرارة التلدين والوقت. استنتج من البحث أن درجة حرارة التلدين والوقت الأمثلين لعملية فصل غاز الأوكسجين هما ٣٢٠ درجة مئوية و ١٢ ساعة. تم القياس النفاذية والانتقائية عند درجة حرارة التلدين والوقت الأمثلين ليكونا ٠,٣٦ بارار و ١٥,٩، على التوالي.

تم تحضير أغشية البوليمر المخلطة بإستخدام كميات مختلفة من زيف-٨ عند درجة حرارة تلدين ٣٢٠ درجة مئوية وزمن قدره ١٢ ساعة. تم تصنيع بلورات زيف-٨ فائقة الصغر عند درجة حرارة الغرفة. ومن ثم استخدمت طريقة

حيود الأشعة السينية لتقدير متوسط قطر البلورة عند ٢٩ نانوميتر. وجد أن النفاذية زادت من ٠,٦١ الى ١,٨١ بارار عندما زادت النسبة المئوية الوزنية لزيف-٨ داخل أغشية البوليمر المخلطة من ٥% الى ٤٠%، بينما ظلت الإنتقائية كما هي. لتحسين أداء عملية فصل الغاز بصورة أكثر، تم تلدين أغشية البوليمر المخلطة التي تحتوي على ٤٣% وزنا من زيف-٨ عند درجة حرارة ٣٢٠ مئوية لمدة ٢٤ ساعة. وجد عندها أن النفاذية والانتقائية ذوي قيمة 1.11 بارار و ١١,٨6 على التوالي، متجاوزين الحد الأعلى لمقياس روبيسون. كما تم معالجة أغشية البوليمر المخلطة كيميائيا بإستخدام الإيثانول والإيثيلين جلايكول، وأظهرت النتائج انخفاض في أداء عملية فصل غاز الأوكسجين عن النتروجين.

CHAPTER 1

INTRODUCTION

Membrane technology, now-a-days is a dynamic and rapidly growing field for gas separation [1]. It is applicable in various gas pair separation processes such as O_2/N_2 separation for oxygen enriched air, CO_2/CH_4 separation in natural gas purification, CO_2/H_2 separation in purification of synthesis gas, H_2/N_2 separation in ammonia purge gas [2]. In this process, gas components are separated from their mixture by differential permeation through a membrane. Membrane based Gas separation process has many advantages such as low capital and operating cost, energy efficiency and easy to scale up. [2-5]. Hence, it has gained significant importance in chemical industry over other conventional techniques such as Pressure Swing Adsorption (PSA) and Cryogenic distillation [6, 7].

1.1.Air (O_2/N_2) Separation overview

Separation of air to produce enriched Oxygen or Nitrogen has been of great significance to the chemical industry. The total membrane market for gas separation is expected to reach $760 million by 2020, and Air separation by membranes represents about $155 million of the overall membrane gas separation business [8]. Oxygen-enriched air is generally used in medical, chemical and industrial applications such as combustion enhancement in furnaces, fuel cells, medical respiration and sewage treatment plants. The small difference between kinetic diameters of nitrogen (N_2, 3.64 Å) and oxygen (O_2, 3.46 Å) molecules makes air separation very difficult by simple size-based diffusion rate differences [9].

1.2. Membrane Technology for Air separation

Over the past few decades, attempts have been made to get oxygen enriched air (OEA) from air. The first successful attempt was made by Ward and Hedman who used silicone rubber to get O_2 from air which was due to the high permeability of polymer and moderate selectivity of O_2 over N_2 [10].

However, a breakthrough in membrane materials and structures could enable the applications of membranes for O_2 enriched air. The present O_2/N_2 separation factor for the commercially available polymer membranes worldwide is in the range of 6 to 8. The scope of O_2 enrichment can be widened considerably if new membranes yielding high separation factors could be synthesized. The practicality of membrane-based O_2 production depends strongly on improvements in membrane performance. Various approaches of using membranes that rely on selectively permeating O_2 with rejection of N_2 have been investigated and recent work on Mixed Matrix Membranes has been fascinating and found to surpass Robeson upper bound [9].

1.3. Background for Membrane based Air separation

Membrane is a selective barrier between phases. The feed gas is passed across the membrane surface at a certain pressure, which is the driving force. The gas that is more permeable penetrates through the membrane and comes out as a low-pressure stream called ‘Permeate’. The remaining gas exiting as a high-pressure stream is called ‘Retentate’. Based on the application and purity, either permeate or retentate, or both streams, can be products. A typical gas separation membrane is schematically depicted in Fig. 1.

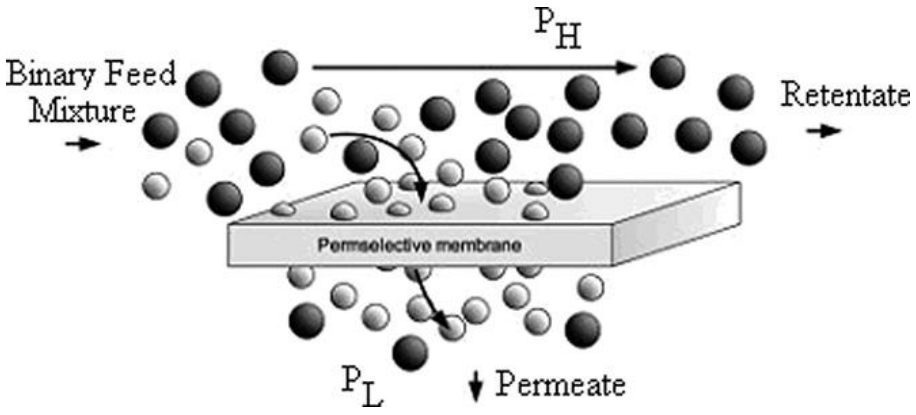

Figure 1: Schematic diagram of gas separating polymer membrane [9]

The two common properties used to describe the O_2/N_2 gas separation performance of membranes are 'Permeability' and 'Selectivity'.

According to the solution diffusion model, the permeation of molecules through membranes is controlled by two important parameters, Diffusivity (D) and Solubility (S).

The **Diffusivity (D)** may be defined as the ability of gas molecules to pass through the voids present between polymer chains in a membrane. **Solubility (S)** may be defined as the ratio of dissolved gas concentration in polymer membrane to the partial pressure of gas.

Thus, **Permeability (P**) of a polymer is defined as the ability of gas molecules to pass through the polymer membrane and is given by the product of Diffusivity (D) and Solubility coefficients (S) as shown in Eqn. (1).

$$\mathbf{P = D * S} \qquad \mathbf{(1)}$$

Permeability, P_x, of a gas 'x' through a membrane could be calculated based on the flux measurements by Eqn. (2):

$$\mathbf{P_{x=}\frac{Q_x L}{\Delta P A}} \qquad \textbf{(2)}$$

Where $\mathbf{Q_x}$ is the volumetric flow rate of gas 'x' at standard temperature and pressure, $\Delta\mathbf{P}$ is the trans-membrane pressure drop, **L** is the effective thickness of the membrane and **A** is the surface area of the membrane. The permeability unit is usually given in Barrers, Eqn. (3).

$$\mathbf{1\ Barrer} = \frac{\mathbf{10^{-10} cm^3 STP.cm}}{\mathbf{cm^2.s\ cmHg}} \qquad \textbf{(3)}$$

The permeability of a membrane is a function of membrane properties (physical and chemical properties), the nature of the permeating gas (size, shape, and polarity) and the interaction between membrane and permeant [11].

Membrane selectivity or perm-selectivity (α) is defined as the ability of a membrane to separate two molecules (in our case, O_2 and N_2) and is given by the ratio of their respective permeability as represented in Eqn. (4).

$$\boldsymbol{\alpha = P_{O2}/P_{N2}} \qquad \textbf{(4)}$$

A higher permeability reduces the membrane area required for separation (hence decreasing the capital cost for membrane units), while high selectivity results in a product with higher purity [12]. Hence in order to achieve an effective gas separation, high permeability and selectivity is required [3].

1.4. Polymeric Gas separation Membranes

Polymeric materials are dominant membrane materials in gas separation due to their desirable properties such as good mechanical properties, low cost, ease of fabrication and environment friendliness [13-15]. Many different polymer families have been investigated as gas separation materials, including polycarbonates, polyesters, polysulfones, polyimides, and polypyrrolones [13, 14, 16]. Polyimides are one class of high performance polymers that have received considerable attention owing to their excellent thermal and chemical stability and high intrinsic separation efficiencies [17-19].

However, Polymeric membranes suffer from a trade-off between their productivity, or permeability, and separation efficiency, or selectivity. This was illustrated by Robeson in 1991 where he plotted polymer selectivity versus permeability in what has become known as the, 'Prior Upper Bound' [20]. Later, the upper bound line was re-drawn in 2008 by updating plenty of data available and named as 'Present Upper Bound' as shown in Fig. 2. The present upper bound correlation can be represented by Eqn. (5)

$$\mathbf{P_i = k * \alpha_{ij}^{n}} \qquad \mathbf{(5)}$$

Where $\mathbf{P_i}$ is the permeability of more permeable gas ; $\boldsymbol{\alpha_{ij}}$ is selectivity / separation factor ; **n** is the slope of log-log plot = -5.667 and **k** is referred as front factor = 1,396,000 [21].

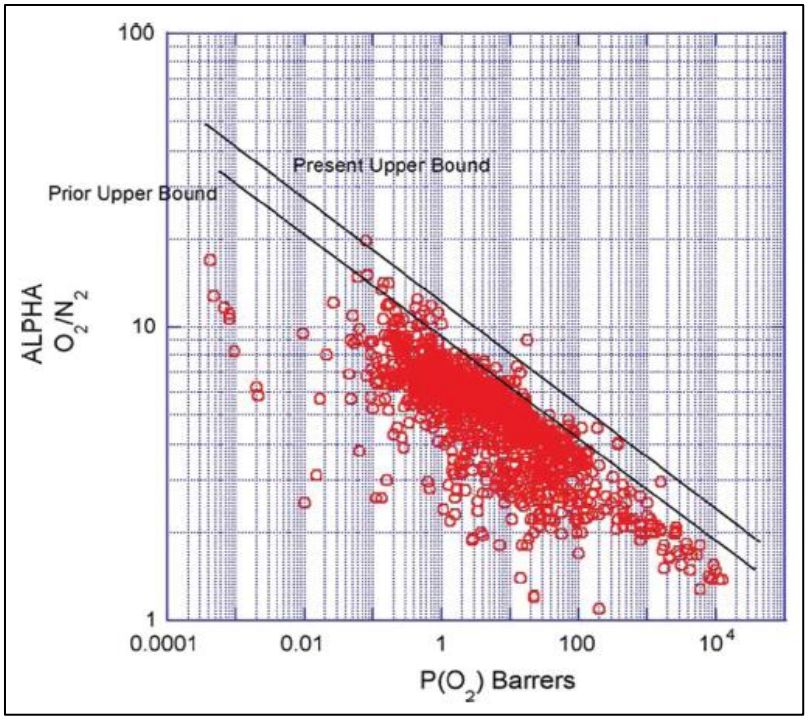

Figure 2: Upper bound correlation for O_2/N_2 separation [21]

1.5. Inorganic Membranes

The inorganic membranes studied so far can be broadly classified into two types, Porous and Non-porous membranes [14]. Porous inorganic membranes include Carbon Molecular Sieves (CMS), Zeolites, Metal Organic Frameworks (MOFs) and Zeolitic Imidazole Frameworks (ZIFs) in which gas separation takes place by the difference in size and shape of permeating gas molecule (i.e., they act as Molecular sieves) and they are known to surpass Robeson upper bound curve [22-35]. On the other hand, Silica, Titanate (TiO_2) and Fullerene (C_{60}) are non-porous inorganic membranes in which the diffusion of larger sized gas molecule is decreased for gas separation [15, 35-45].

Thus, Porous inorganic membranes can be more favorable for gas separation due to their high permeability, selectivity, thermal and chemical stability properties. Nevertheless they

are limited by high fabrication costs, low reproducibility, low mechanical resistance and brittleness [21, 25].

1.6. Mixed Matrix Membranes (MMMs)

For gas separation applications, the polymeric membranes have been researched extensively and they have attained the upper bound limit in the trade-off line. Inorganic membranes have good thermal stability, chemical stability and high permeability and selectivity. However, the inorganic membranes are limited by fabrication costs. Therefore, to overcome these limitations of polymer and inorganic membranes, a new membrane called Mixed Matrix Membrane (MMM) has become an important research issue in recent years [20, 46]. Mixed matrix membranes contain a continuous "Polymer phase" and a dispersed "Inorganic filler phase" as shown in Fig. 3 [2]. They theoretically combine the advantages of both polymers (processibility, low cost etc.) and inorganic membranes (separation performance) [47]. Properties of mixed matrix membrane can be affected by particle size, pore size, loading amount of inorganic material and properties of polymeric materials [15, 48].

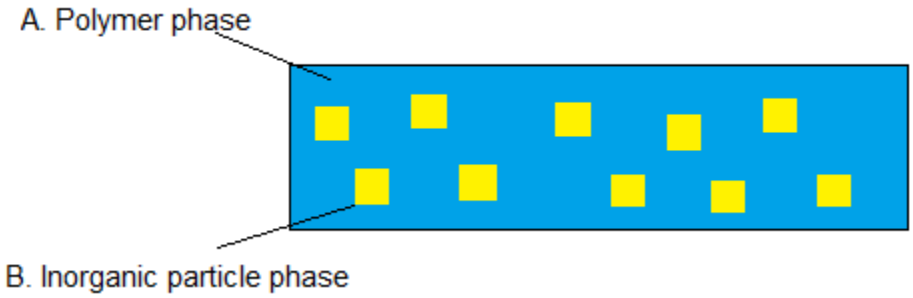

Figure 3: Schematic diagram of Mixed Matrix Membrane (MMM)

1.7. Motivation

For MMM preparation with good gas separation performance, a suitable combination of polymer and inorganic filler is very important. A polymer with high selectivity and filler with high permeability is found to be the most suitable combination for MMM development [14]. Hence, polyimide Matrimid 5218 which is a commercially available gas separation polymer is selected as it exhibits high selectivity (6-7). ZIF-8, a subclass of MOFs, has great potential for gas separations and it is known for retaining selectivity of polymer and increasing the permeability significantly when used for MMM fabrication. Hence, ZIF-8 is selected as inorganic filler phase.

The work done on Matrimid/ZIF-8 MMMs for O_2/N_2 gas separation in the literature so far shows that the performance is below Robeson upper bound. Song et. al prepared Matrimid/ZIF-8 MMMs and studied annealing effect up to 230°C. They annealed a 20 wt% MMM from 60 to 230°C for 18 hours under vacuum and found that selectivity increased continuously from 2.2 to 6.4. Due to this continuous improvement with annealing temperature, it is worth trying higher temperatures than 230°C and closer to the glass transition temperature of Matrimid (Tg = 317°C). It is believed that at temperatures close to Tg better molecular packing can be achieved with annealing, hence, higher selectivity can be achieved.

1.8. Objectives

The main objective of the present work is to enhance O_2/N_2 gas separation performance of Mixed Matrix Membranes prepared by varying ZIF-8 composition in Matrimid polymer.

The specific objectives of this work are:

1. To synthesize ZIF-8 crystals at room temperature.

2. To study the effect of annealing temperature and time (Post Heat treatment) on O_2/N_2 gas separation performance of Pure Matrimid polymer.

3. To study the effect of ZIF-8 filler loading percentage on the O_2/N_2 gas separation performance of the developed Mixed Matrix Membranes.

4. To study the effect of annealing temperature (Post Heat treatment) and Chemical Treatment on the O_2/N_2 gas separation performance of the MMMs.

CHAPTER 2

LITERATURE REVIEW

2.1. Polymer Membranes

A Membrane can be described as a barrier between two phases through which transport can take place due to the difference in pressure or concentration. In principal, all materials that can form thin and stable films can be used as Membranes.

Synthetic polymeric membranes are fabricated in two main geometries:

1) Flat sheet - Used in the construction of flat sheets, discs, plate, and frame modules

2) Cylindrical - Used in tubular and hollow fiber modules.

Gas separation is possible due to the differences in transport rates of gases in a gas mixture, the gas which diffuses fast becomes enriched in permeate side while the gas which diffuses slowly gets accumulated on the retentate side of the membrane. Porosity is also an important factor for gas separation, lesser the size better the separation. Based on the pore size and flux density, Polymer membranes can be classified as 1) Porous (or) Rubbery Polymers, 2) Non-porous (or) glassy polymers and 3) asymmetric [49].

2.1.1 Rubbery Polymers (or) Porous membranes

A porous membrane is rigid membrane and it has well-defined pore structure and have pores in the range of 5-100 nm. Rubbery polymers are flexible and soft, and they operate above their Glass Transition temperature (Tg). They exhibit high intra-segmental mobility and short relaxation times. Gas separation in a porous membrane is dependent on various

parameters such as size of pores in the membrane and pore distribution. Porous membrane acts as a conventional filter which can separate gas molecules differing in size. Porous membranes generally exhibit high permeability but low selectivity.

Porous membranes can be divided into three types depending on the size ranges of their pores, macroporous (>50 nm), mesoporous (2-50 nm) or microporous (<2 nm) [50]. They can be prepared by various methods such as solution casting, sintering, phase separation, track etching and the final morphology of polymeric membrane depends on the materials used and processing conditions [51]. For example, Silicone rubber and Polydimethylsiloxane (PDMS) are considered to be porous membranes.

2.1.2. Glassy Polymers or Non-porous Membranes

Glassy polymers are glass-like and rigid and they operate below their glass transition temperatures (Tg). They have low chain intra-segmental mobility and long relaxation times. Non-porous membranes also called as dense membranes have high selectivity but low permeability. Non-porous membranes can separate gases of even similar atomic sizes if their solubilities in the membrane are significantly different. These non-porous membranes can be prepared by melt-extrusion or solution casting [52]. Polyimides, Polycarbonates, Polysulfones, Polycarbonates, Polyethene, Cellulose Acetate are few examples of Glassy polymers.

2.1.3. Asymmetric membrane

These are the most used membranes in industries. Asymmetric membranes consists of generally two layers, first one is a ‘dense skin layer’ which is very thin while the second one is a thick ‘porous layer’. The first layer controls the performance of the membrane by

considering permeation properties while the bottom layer provides support and strength to the membrane. Thin film composites and integrally skinned are two general classes of Asymmetric membranes. If the top and bottom layer are of same material then it is referred to as 'Integrally skinned Asymmetric Membrane' (as shown in Fig.4) but if the top layer and bottom layer in a asymmetric membrane are of different material then it is named as a 'Composite Asymmetric Membrane'. Composite Membranes have advantage over Integrally skinned Membrane as one can choose different top and bottom layer thus optimizing the permeation properties of the membrane [52].

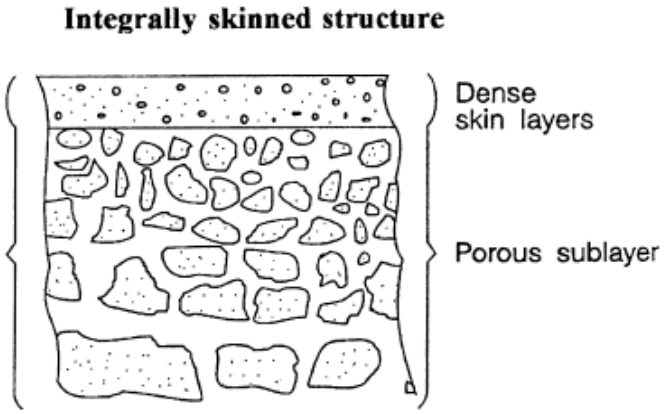

Figure 4: Schematic diagram of Integrally skinned Asymmetric Membranes [53]

2.2. Methods for the Membrane fabrication

Different methodologies are available to prepare membranes. A brief description of some the common methods for membrane fabrication such as phase inversion process, sintering of powders, stretching of films, and dip coating are discussed. The most common method for preparing non-porous membranes (Matrimid, in the present study) is solution casting and solvent evaporation [49, 53].

2.2.1. Phase inversion

It is a process in which a polymer changes its state from liquid to solid in a controlled way. This solidification process starts when the high polymer concentration liquid phase transforms itself into a solid matrix. By controlling the initial stage of this phase transformation, either porous or non-porous membrane can be prepared.

Different techniques employ the concept of phase inversion such as solvent evaporation, immersion precipitation, precipitation by controlled evaporation, thermal precipitation, and precipitation from vapor phase. Some of these phase inversion techniques are discussed here.

(a) Solution Casting and Solvent Evaporation

This method produces a dense symmetric membrane and is the simplest of all techniques. Bubble-free and sufficiently viscous polymer solution is cast on a suitable flat surface (usually, glass plate of petri-dish), as shown in Fig. 5. The thickness of the membrane is controlled by the viscosity of the polymer solution. After casting the solution, the solvent is evaporated to leave a thin and uniform polymer film. High-boiling solvents are inappropriate for this method, because their low volatility demands long evaporation time [53].

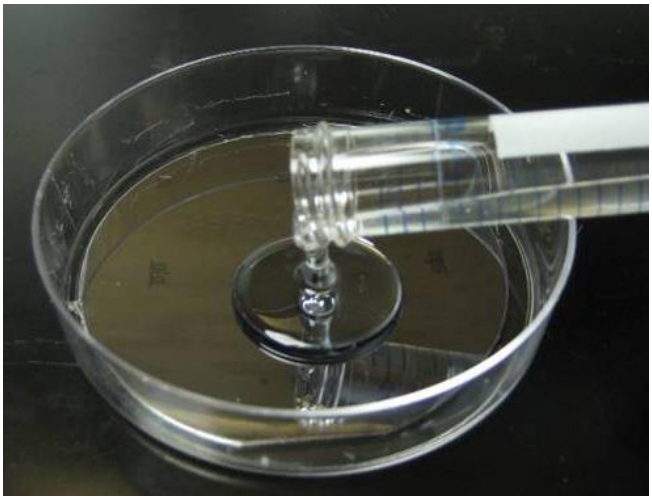

Figure 5: Solution casting method using petri-dish

(b) Immersion Precipitation

In this method, a polymer dissolved in a suitable volatile solvent and it is cast on a plate by a doctor's blade. After partial evaporation of solvent, the polymer film is immersed in a gelation bath which is a non-solvent medium. Solidification of the film occurs as a result of mass transfer and phase separation and is described by the following two-step process:

I) Evaporation of the solvent takes place and a non-porous thin layer of polymer is formed at the top of the film instantly.

II) Solvent – non solvent exchange in the gelation bath: The excess non solvent diffuses into the polymer solution film via the thin polymer layer, as the solvent diffuses out forming a porous layer. The upper skin layer can be made porous by decreasing the polymer concentration in the casting solution or by using a less volatile solvent such as dimethyl form amide [9].

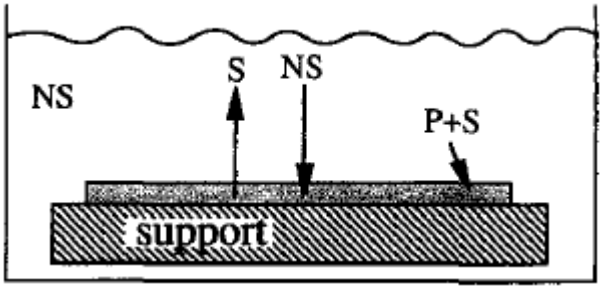

Figure 6: Schematic Diagram of Immersion precipitation [53]

(c) Precipitation by Controlled Evaporation

In this method, polymer is dissolved in a mix of solvent and non-solvent. As solvent is more volatile than non-solvent, it evaporated and thus leading to the precipitation of the polymer and formation of thin polymer membrane.

(d) Thermal Precipitation

In this case, Polymer membrane is prepared by mixing the polymer with a substance that acts as a solvent at high temperature and casting the solution into a film. When the solution is cooled, solidification occurs. This method is generally used for microfiltration. For example, Polyvinylidene Fluoride (PVDF) membranes were prepared by dissolving in N-Methyl-2-pyrrolidone (NMP) solvent at 40°C for 24 h and then casting [54].

(e) Precipitation from vapor phase

In this method, solvent-polymer mixture is cast on the film. Then it is placed in vapor atmosphere which contains non-solvent saturated with the same solvent. Due to the high concentration of solvent in the vapor atmosphere, the solvent from the cast film stays instead of evaporating into the atmosphere. Membrane formation takes place by the diffusion of non-solvent into the cast film and a porous membrane is formed [9]. For

example, poly(vinylidene fluoride) (PVDF) membranes were prepared using DiMethylFormamide (DMF) as solvent and water as non-solvent. [55]

2.2.2. Sintering

Sintering is one of the simplest techniques and is used for preparation of porous membranes either from organic or inorganic materials. In this technique, a polymer (in the form of powder) is compressed and later sintered at an elevated temperature (below melting point of polymer). The sintering temperature depends on the material used. During the process of sintering, the interface between particles in contact disappear and a pore is formed as shown in Fig. 7.

Figure 7: Schematic diagram showing the pore formation in sintering process [53]

The pore size of the sintered membrane depends on the size of the particle and its distribution in powdered polymer material. The resultant product of sintered powder have porosity in the range of 10-20% and pore size in the range of 0.1 – 10 μm [53].

2.2.3. Stretching

This technique is used to prepare microporous membranes. They are prepared by stretching a partially semi-crystalline polymer (such as: Polypropene, Polyethene, Poly Tetra Fluoro Ethelyne] perpendicular to the direction of extrusion. Polymer powder is extruded at a temperature close to its melting point with a rapid draw-down to obtain thin film and crystallites areas which are aligned parallel to the extrusion direction. After annealing and

cooling, a mechanical stress is induced which causes small pores in the range of 0.1-3 μm [53].

2.2.4. Dip Coating

Dip coating is used to prepare composite membranes with thin top layer and is a relatively simple technique. In this method, porous substrate (flat sheet or hollow fiber) is dipped in the solution containing the polymer in an appropriate solvent. When the substrate is removed from the coating bath, a thin layer of solution adheres on it, which contains both polymer and solvent. This thin film is then put in an oven to evaporate solvent and forms a composite membrane, and sometimes, based on the polymer, cross-linking also occurs while heating [9].

2.3. Gas Transport Mechanisms of membranes

The gas transport in polymer membranes is mainly dependent on the polymer properties, such as composition, free volume content, crosslinking, average molecular weight, molecular weight distribution, intersegmental chain spacing, polymer polarity, defects, thermal processing history, degree of crystallization, glass transition temperature, and morphology [56]. The gas transport mechanism varies depending on the type of membranes i.e., porous or non-porous [52].

2.3.1. Gas transport in porous membranes

Gas transport in porous membranes occurs depends on pores size. So, for different pore sized membranes the mechanism of transport varies [52, 56]. The mean free path (λ) of a

gas molecule is defined as the average distance travelled by the molecule between collisions and is given by the Eqn. 6 [57].

$$\lambda = \frac{3\eta}{2P}\frac{(\pi RT)^{1/2}}{2M} \qquad (6)$$

where η is the viscosity of the gas, R the universal gas constant, T the temperature, M the molecular weight, and P the pressure.

For porous membranes, the most common mechanisms are:

(a) Molecular diffusion (Poisseuille flow / Laminar flow)

If the mean free path of the gas molecule (λ) is less than the pore size of membrane (r) then diffusion mainly occurs through inter-molecule collisions and is called Molecular diffusion. In this type of diffusion, the driving force is the composition gradient. If the membrane is subjected to pressure gradient then laminar flow occurs and such transport is called Poisseuille flow (or laminar flow) and is shown in Fig. 8 [52].

(b) Knudsen diffusion (Viscous flow)

This mechanism is common in case of macroporous and mesoporous membranes. The gas transport occurs via Knudsen diffusion if the mean free path of the gas molecule (λ) is greater than pore size of the membrane (r). In this case, the collisions of gas molecules with pore wall of membrane will be more frequent than the collision among molecules as shown in Fig. 8. In this mechanism, the selectivity of membrane to separate gases is proportional to the ratio of inverse square root of the molecular weights [52, 56, 57].

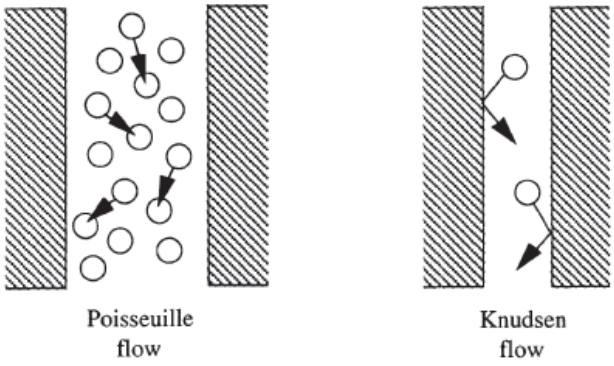

Figure 8: Schematic diagram showing Poisseuille flow and Knudsen flow [53]

(c) Molecular sieving (or surface diffusion)

In this mechanism, gas separation occurs when the pore size of the membrane is similar to the size of permeating gas molecules. In this case, only smaller molecules can permeate and a very high selectivity would be achieved. This mechanism is prevalent in Zeolites and Carbon Molecular Sieves (CMS) [52].

(d) Capillary condensation

In this mechanism, partial condensation a gas molecule takes place in the pores followed by transport of condensed molecule across the pore. Hence, a layer of condensable gas would form which will prevent the flow of non-condensable gas and this can be used to achieve very high selectivities [52].

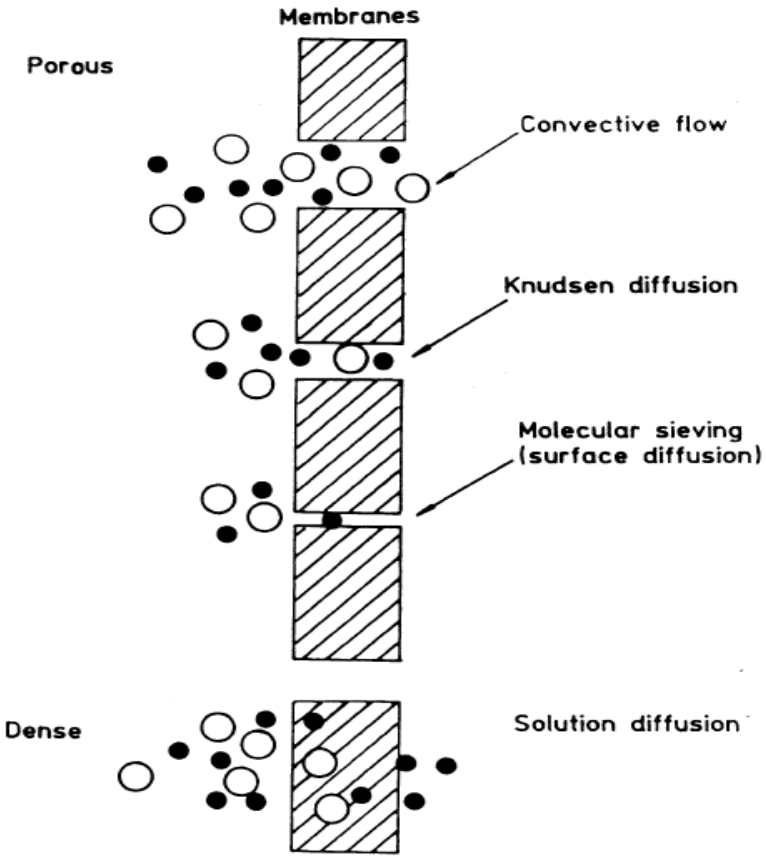

Figure 9: Schematic showing various gas transport mechanisms in membranes [56]

Among all the mechanisms mentioned above, Knudsen mechanism gives low selectivity for gas separation while Molecular sieving mechanism shows high selectivity and permeability for smaller sized gas molecules [52].

2.3.2. Gas transport in Non-porous membranes

Solution-diffusion is the mechanism of gas transport in the non-porous membranes made of glassy polymers. It is based on two essential parameters, solubility of molecule and mobility of molecule. Diffusion selectively permeates smaller gas molecule while solubility factor permeates the more condensable gas species [58]. This mechanism of gas transport can occur in a three step process as shown in Fig. 10 and is described as follows:

1) In the first step, the gas molecules are absorbed by the membrane surface on the upstream end (Absorption).

2) Then in the second step, diffusion of gas molecules occur though the polymer membrane (Diffusion).

3) Finally, the gas molecules evaporate on the downstream end (Desorption).

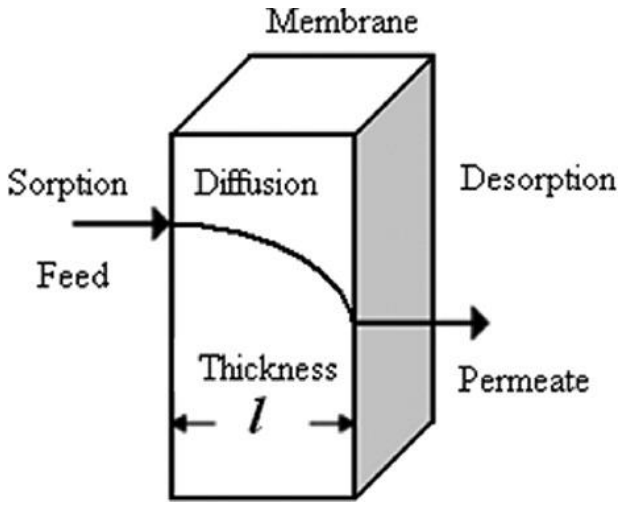

Figure 10: Solution diffusion Mechanism in Non-porous membranes [9]

The first step, sorption of gases, is a complex process in case of glassy polymers. it is named as "dual mode sorption theory" and described by the combination of Henry's law and Langmuir expressions [52, 59]. Solution–diffusion mechanism is driven by a difference in the thermodynamic activities causing a concentration difference which leads to the diffusion in the direction of decreasing activity. This model assumes that the pressure within a membrane is uniform and that the chemical potential gradient across the membrane is expressed only as a concentration gradient [52, 59].

The rate determining parameter is the permeability (P), which is given by the product of a solubility coefficient (S) and a diffusion coefficient (D) i.e., **P = D * S**

2.4. Selection of Polymer and Filler Material

For MMM preparation with enhanced gas separation performance, a suitable combination of polymer and inorganic filler is very important [47, 60-62].

The selection of polymer and filler material can be visualized in a qualitative way. If the permeability of polymer is significantly higher than the inorganic filler then, gas transport occurs only through the polymer as it is the least resistant path, leaving the filler phase futile and hence the filler can't contribute to the gas separation performance [14]. Therefore, a polymer with high selectivity and low permeability is found to be most suitable for MMM development [14]. Hence, polyimide Matrimid®, which is a commercially available gas separation polymer, is selected as it exhibits high selectivity [63] . The filler should have high permeability and most important is that MMM should retain the selectivity of polymer to a maximum extent. ZIF-8 has high permeability for O_2 (~ 400 barrers), hence it is selected as inorganic filler phase [25, 64]. The chemical structures of Matrimid and ZIF-8 are shown in Fig. 11.

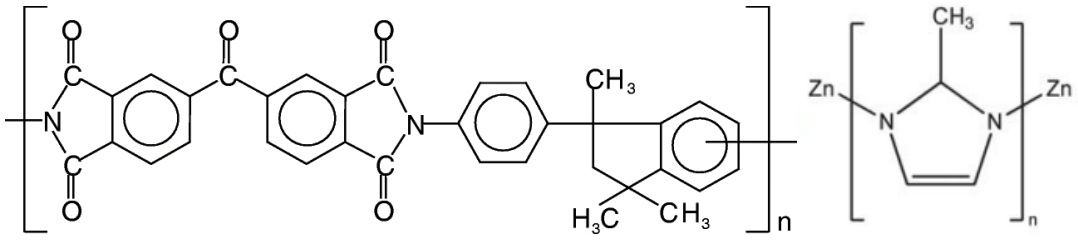

(a) (b)

Figure 11 : Chemical Structures of (a) Matrimid and (b) ZIF-8 [64, 65]

2.4.1. Matrimid 5218

Matrimid 5218 is a commercially available polyimide and is widely used for Gas separation applications. Matrimid is composed of 3,3`,4,4`-Benzophenone tetracarboxylic dianhydride (BTDA) and diaminophenylindane (DAPI) [65]. There has been significant research on Matrimid 5218 polymer membrane for O_2/N_2 gas separation as shown in Table 1.

Table 1 : Literature Review of O_2/N_2 gas separation performance for Matrimid and various MMMs

S.No.	Polymer/MMM	Permeability	Selectivity	Ref
1	Pure Matrimid	2.65	6.17	[66]
	Matrimid/Zeolite-4A (30 wt%)	11.1	5.36	
2	Pure Matrimid	1.5	6.88	[67]
	Matrimid/ Zeolite-13X (43 wt%)	6.58	4.87	
3	Pure Matrimid	1.29	5.86	[43]
	Matrimid/TiO2 (25 wt%)	3.25	1.78	
4	Pure Matrimid	1.7	6.6	[68]
	Crosslinked with p-xylenediamine	1.9	6.5	
5	Pure Matrimid	1.7	6.8	[69]
	Crosslinked with EDA	0.587	8.51	
	Crosslinked with BuDA	1.14	7.65	

Ahmad et.al [66] have prepared Matrimid/Zeolite4A MMM for O_2/N_2 gas separation and they have studied the effect of Zeolite loading on MMM, effect of operating temperature, effect of feed pressure and effect of Membrane annealing temperature. They have found that as the Zeolite 4A loading was varied in MMM from 0 to 30 wt%, permeability was found to increase from 2.65 to 11.10 barrers while Selectivity decreased from 6.17 to 5.36. As the operating temperature was varied from 30 to 70 °C, the permeability of O_2 increased from 2.65 to 7.10 barrers while selectivity decreased significantly from 6.17 to 2.26. The feed pressure was also changed from 2 to 8 bars and it was found that there was negligible

change in permeability and selectivity. The annealing of MMM at 250 °C for 3 h was found to enhance O_2/N_2 gas separation properties. MMM (30wt% Zeolite 4A) dried at room temperature had permeability of 12.8 barrers and selectivity of 4. On the other hand, when MMM was annealed at 250°C, it resulted in decrease of permeability to 11.0 barrers and selectivity increased to 5.36, thus improving the gas separation performance slightly.

Yong et.al [67] developed Matrimid/Zeolite 13X MMMs for O_2/N_2 gas separation. Zeolite molecular sieves are highly porous materials from the family of aluminosilicates. Depending on the type of molecular sieve type and pore size, various zeolites are designated. Zeolite 13X has pore opening of 8 A^o and has molecular sieve type "X". They studied the effect of Zeolite 13X loading on the Gas separation performance of MMM. They found that as the loading % was changed from 0- 43wt%, the permeability increased from 1.5 to 6.58 barrers while selectivity decreased from 6.88 to 4.87.

Moghadam et.al [43] developed Matrimid/TiO_2 MMMs for O_2/N_2 gas separation and they studied the effect of TiO_2 loading on the Gas separation performance of MMM. They found that as the loading % was changed from 0 to 25wt%, the permeability increased from 1.29 to 3.25 barrers while selectivity decreased from 5.86 to 1.78.

Tin et.al [68] studied the effect of room temperature crosslinking on O_2/N_2 gas separation performance of Matrimid 5218 membrane. They prepared Matrimid polymer membrane and crosslinked it using a crosslinking reagent with 10% (w/v) p-xylenediamine in methanol and various immersion times (0 -32 days). They observed that among all the immersion times, 1 day immersion time showed better separation properties [Permeability increased slightly from 1.7 to 1.9 barrers while selectivity decreased from 6.6 to 6.5].

Shao et.al [69] also studied the effect of crosslinking on O_2/N_2 gas separation performance of Matrimid 5218 but with various diamines such as ethylenediamine (EDA) and 1,4-butane diamine (BuDA). Each of the diamines was treated with Matrimid polymer membrane for 3 h and the permeabilities were tested. They found that both of them showed an increased selectivity with a slight decrease in permeability. EDA treatment resulted in increase in selectivity from 6.80 to 8.51 while permeability decreased from 1.7 to 0.587 barrers. Similarly, BuDA treatment resulted in improved selectivity from 6.80 to 7.65 while permeability decreased from 1.70 to 1.14 barrers.

2.4.2. Zeolitic Imidazolate Framework-8 (ZIF-8)

One of the most studied ZIFs is ZIF-8 which is made up of Zn tetrahedral clusters and 2-Methyl imidazolate linkers and prepared using zinc hexanitrate and 2-methyl imidazole. It has the sodalite (SOD) type of zeolite structure and forms a truncated octahedron shown in Fig. 12. These join together to make an extended 3D framework as seen in Fig. 8. ZIF-8 was first reported by Yaghi et al using solvothermal synthesis in 2006 [70].

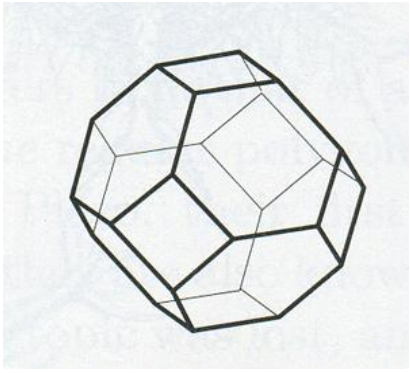

Figure 12 : Sodalite unit cell forming a truncated octahedron

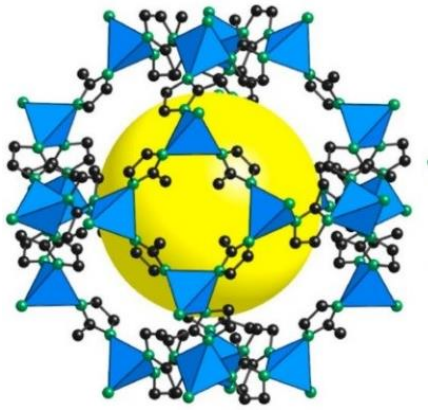

Figure 13 : Structure of ZIF-8, yellow sphere indicate the pore volume [35]

ZIF-8 has pore-diameter of 11.6 Å and pore-opening of 3.4 Å due to the methyl side chains on the imidazolate linkers. This gives them pore sizes approximately double that of zeolites, as the imidazolate linker is longer than that of the bridging oxygens in zeolites, but apertures that are comparable to the smallest of molecular sieves. The surface area of ZIF-8 is very high, nearly 900-1600 m^2/g [70]. They also have high thermal stability (up to 550 °C) and outstanding chemical resistance to organic solvents [35]. It is expected that ZIF-8 nanoparticles yield better contact with polymer matrix and reduction in interfacial voids due to their large surface area [71, 72].

Many studies have been published reporting the synthesis of ZIF-8 crystals using different solvents (i.e. methanol, dimethyl formamide (DMF), diethylformamide (DEF), water) by solvothermal and rapid mixing methods. Synthesis temperatures have changed between room temperature and 140^0C, and the synthesis time was between 5 minutes and 1 month [25, 73, 74].

Due to its wide range of potential applications, some studies aimed for production of nanometer sized ZIF-8 crystals and some investigations tried to control the crystal size.

For example; Balkus et al. synthesized ZIF-8 crystals using traditional solvo-thermal method at 140^0C for 6-8 hours by using DMF as the solvent [25]. They obtained 50 to 150 nanometer-sized crystals with a BET surface area of 1300 m^2/g so as to use in fabrication of mixed matrix membranes. They achieved the Nano sized crystal synthesis by adding a base into the synthesis solution.

Cravillon et al. reported the ZIF-8 crystals synthesized in 1 h in methanol at room temperature with 50 nm crystal size [75]. They controlled the ZIF-8 nano- and microcrystal formation by employing an excess of the bridging bidentate ligand and various simple auxiliary monodentate ligands with different chemical functionalities (carboxylate, Heterocycle, alkylamine). They also found that using excess of Methanol (e.g. 1500 moles instead of 1000 moles) resulted in smaller crystal size of ZIF-8.

Venna et al.[76] reported synthesis of ZIF-8 in the presence of excess solvent (i.e., methanol) at room temperature. Structural evaluation of ZIF-8 was studied as a function of time and evaluation of the crystal size and extent of crystallinity were analyzed. They found that at 5 min stirring time, small spherical shaped ZIF-8 nanocrystals formed while after 24 hours of stirring, large rhombic dodecahedral shaped particles were formed.

Pan et al.[74] reported the rapid synthesis of ZIF-8 nanocrystals being between∼50 and 85 nm in size. But they used deionized water instead of Methanol as solvent and a much larger excess of the bridging Hmim ligand (Hmim/Zn > 70:1).

It can be inferred that by using the stirring time of 5 min and excess of Methanol [Zn : Hmim: MeOH =1:4:1500], ZIF-8 particles with minimum crystal size (20-30nm) can be prepared.

2.5. ZIF-8 based Mixed Matrix Membranes

In literature, the usage of ZIF-8 crystals as a filler in MMMs has become an important research topic in recent years, due to its promising molecular sieve performances. There are limited numbers of research for ZIF-8 loaded MMMs in literature, and their results are presented in Table2 and their permeability versus selectivity plot is shown in Fig. 14.

Table 2 : Literature Review of O_2/N_2 gas separation performance for various Membranes related to ZIF-8 (pure and MMMs)

S.No.	Polymer or MMM	O_2 Permeability	Selectivity	Ref
1	ZIF-8	468	1.80	[77]
2	PIM-1	580	3.22	[78]
	PIM-1/ZIF-8 (43wt%)	1680	4.80	
3	Matrimid , 230 °C	2.62	7.30	[64]
	Matrmid/ZIF8 (30 wt%)	10.18	6.1	
4	Matrimid, 240 °C	1.98	6.60	[25]
	Matrmid/ZIF8 (40 wt%)	5.88	5.60	
5	PPEES	1.28	5.57	[79]
	PPEES/ZIF8 (30wt%)	12.12	5.18	
6	PSF	1.4	5.60	[80]
	PSF/ZIF-8 (16wt%)	2.6	8.30	

Bushell et al. [78] prepared and studied Mixed Matrix Membrane with ZIF-8 as inorganic filler and PIM-1 as polymeric membrane. They found that permeability of O_2 increased 3 times (from 580 to1680 barrers) and selectivity also increased from 3.22 to 4.8 as the wt% of ZIF-8 in MMM was increased from 0 to 43%. The MMM with 43 wt% was found to surpass Robeson upper bound.

Song et.al [64] prepared Matrimid/ZIF-8 MMM and studied the effect of annealing temperature and effect of ZIF-8 loading on O_2/N_2 gas separation performance of MMM. The best performance was observed in MMM with 30 wt% ZIF-8, annealed at 230 °C. The

permeability when compared to pure Matrimid membrane increased 4 times (2.62 to 10.18 barrers) while selectivity decreased from 7.3 to 6.1.

Wijenayake et.al [81] developed 33 wt% ZIF-8 6FDA-durene/ ZIF-8 MMMs and annealed under vacuum at 210 °C for 24 hrs. The permeability of O_2 and N_2 was tested at 3.5 atm and 35°C. They found that the permeability increased by 316%, from 108 to 450 barrers due to the introduction of ZIF-8 in 6FDA-durene. On the other hand, selectivity was found to remain almost the same (3.1 to 3.3).

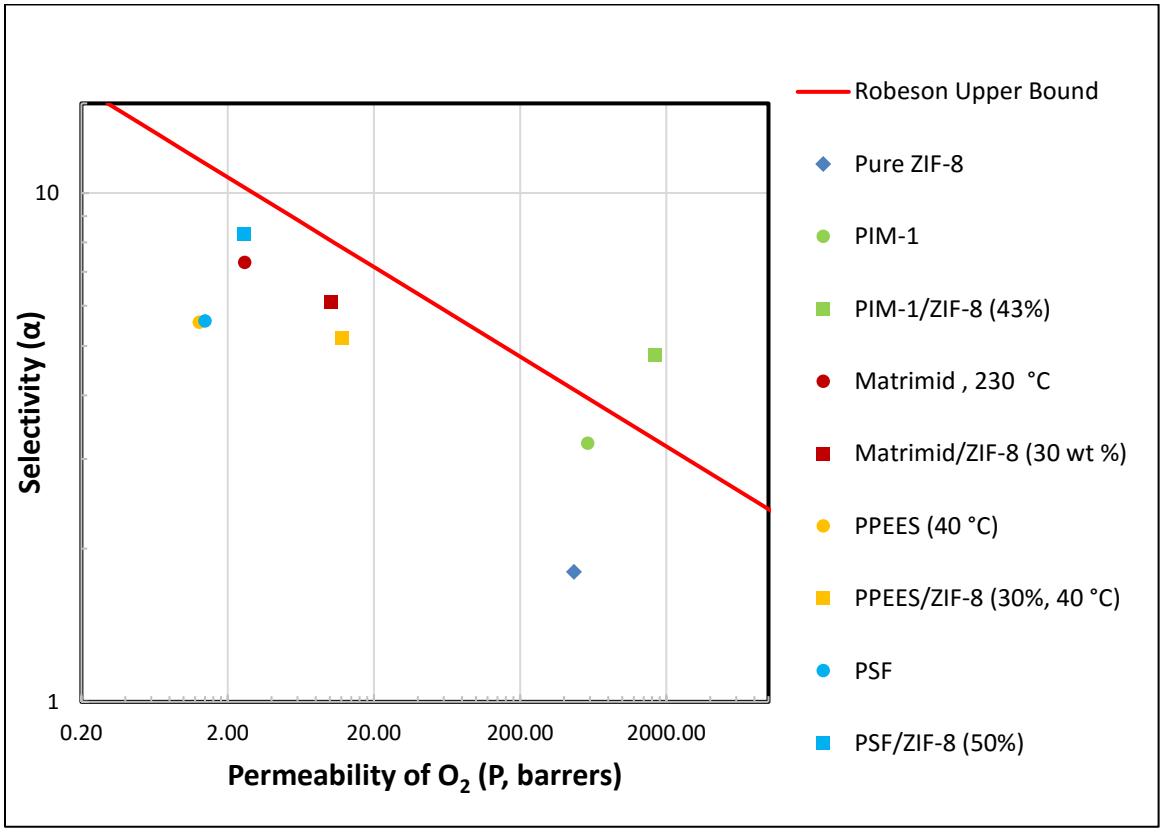

Figure 14 : Permeability Versus selectivity plot of Various ZIF-8 based Mixed Matrix Membranes

Ordonez et al. [25] prepared ZIF-8/Matrimid mixed matrix membranes by varying the loading amounts of ZIF-8 from 0 to 80 wt%. The particle sizes of ZIF-8 crystals

synthesized by hydrothermal process using triethylamine (TEA) as ligand, were in the range of 50 to 150 nm. The permeabilities of O_2, N_2 gases were tested. When ZIF-8 loading was increased from 0 to 40 wt%, the permeability of O_2 gas increased from 1.98 to 5.88 barrers because of the increase in the distance between polymer chains, creating more polymer free volume, while the selectivity decreased slightly.

Diaz et al. [79] studied the effects of ZIF-8 on gas transport performances of hybrid membranes which contained poly(1,4-phenylen ether-ether-sulfone) (PPEES) as polymer matrix. Loading amounts of ZIF-8 particles that have particle size of 4.9 μm were 10, 20 and 30 % (wt/wt). All the membranes were annealed at 20, 30, 40°C respectively and their permeability results of O_2 and N_2 gases were reported. The permeability of O_2 increased up to 10 times (0.88 to 9.23 barrers) with the addition of ZIF-8 (0 to 30 wt %) while the selectivity remained almost the same. They found a marginal improvement in the gas separation performance of MMM which were annealed at 20°C and 40°C. They concluded that the ZIF-8 loading of 30 wt% showed good separation performance due to closeness of its selectivity to the Robeson's upper bound.

Zornoza et al. [80] prepared ZIF-8 based Mixed Matrix Membrane using Polysulfone as the polymer without any interfacial voids and good contact between polymer and filler. They found that Performance of MMM was good and its values were reported close the upper bound. The permeability of O_2 increased from 1.4 to 2.6 barrers while selectivity increased from 5.6 to 8.3 as the loading of ZIF-8 was increased from 0 to 50 wt%.

Diestel et al. [77] fabricated Mixed Matrix Membrane (MMM) with ZIF-8 as filler additive and Poly Methyl Phenyl Siloxane (PMPS) as polymer phase. They also prepared ZIF-8

membrane with alumina support and tested the permeability of O_2 and N_2 in PMPS, ZIF-8 membrane, and MMM. The permeability and selectivity of Pure ZIF-8 membrane was reported to be 468 barrers and 1.8 respectively. Also, with increase in ZIF-8 loading from 0 to 8.3 wt%, the permeability increased three fold while selectivity remained almost the same.

It can be observed from Fig.14 that only one result of ZIF-8 based MMMs surpassed Robeson present upper bound curve which uses PIM-1 as polymer. PIM-1 is very difficult and long process to prepare in lab and is not commercially available. Hence, in the present study, Matrimid is used as polymer which is a commercial polymer.

2.6. Effect of the particle size of filler on the Gas Separation Performance

Numerous researchers have indicated that the permeance performances of MMMs are related to particle shape and size, particle pore size and pore size distribution as well as operating conditions. The permeability behavior depends on particle size of fillers due to changing area of filler-polymer interfaces by number of particles [14, 82].

Huang et al. [83] investigated the effect of the particle size of Zeolite-4A on the permeation performance. MMMs were produced by using micro sized and nanosized Zeolite-4A particles (20 wt % of the polymer) and polyethersulfone that annealed above the Tg of the polymer. The permeabilities for He, H_2, O_2, CO_2, CH_4 and N_2 gases significantly increased when using nanosized Zeolite-4A/PES membrane relative to microsized Zeolite-4A/PES membrane. The permeabilities of all mixed matrix membranes for all gases decreased compared to the permeability of pure PES membrane. Microsized Zeolite-4A/PES

membrane and nanosized Zeolite-4A/PES membrane had same selectivity values for H_2/CO_2 and CO_2/CH_4 gas pairs.

Bushell et al. [78] prepared two different particle sizes of ZIF-8 crystals which had 2-10 μm and 40-60 nm. Gas separation performances were analyzed for ZIF-8/PIM-1 MMMs. The volume percent of filler in the membranes were 11 with microZIF-8 and 16, 28, 36 and 43 with nanoZIF-8. The permeation tests of pure gases such as He, H_2, O_2, N_2, CO_2 and CH_4 were done for prepared ZIF-8/PIM-1 membranes. For nanoZIF-8/PIM-1 membranes, the permeability improved as well as ideal selectivities with addition of nanoZIF-8 particles. Moreover, gas separation performances of both for nanoZIF-8 and microZIF-8 containing PIM-1 membranes shift above the upper bound limit in the trade-off line for several gas pairs.

Dai et al. [84] prepared dual layer composite Ultem 1000 asymmetric hollow fiber membranes with using ZIF-8 as filler. The particle size of ZIF-8 was around 200 nm. The loading of ZIF-8 was 13 wt % in the selective skin layer of the membrane. The permeation tests were done for pure N_2 and CO_2 gases and mixed gas that included 20 % CO_2 in N_2. The permselectivity for CO_2/N_2 was improved as high as 20 % over pure Ultem 1000 hollow fiber membrane when ZIF-8 particles loaded to Ultem 1000 asymmetric hollow fiber membrane. Also, the permeance of pure CO_2 for ZIF-8/Ultem 1000 hollow fiber membrane increased to two times of pure Ultem 1000 hollow fiber membrane.

Keser et al. [85] investigated effects of ZIF-8 loading amount on the membrane separation performances. MMMs were prepared by polyethersulfone (PES) as polymer phase, ZIF-8 as filler and 2-hydroxy 5-methyl aniline (HMA) as LMWA. The particle size of ZIF-8 was

around 60 nm. In binary mixed matrix membranes, ZIF-8 particles were loaded up to 60 % (wt/wt). In ternary mixed matrix membranes, ZIF-8 particles and HMA were loaded up to 30 % (wt/wt) and 10 % (wt/wt), respectively. The permeation tests for pure H_2, CO_2 and CH_4 gases were done at different feed pressures between 3 and 12 bar. When ZIF-8 particles were loaded to pure PES membrane, the permeability values of all gases increased with decreasing ideal selectivities, slightly. PES/ZIF-8(20%)/HMA(7%) was the best membrane composition for separation performance of pure gases among ternary membranes because of improving H_2/CH_4 selectivity, significantly. Also, it was shown that the separation performances of all membranes improved with increasing feed pressure.

2.7. MMMs for O_2/N_2 gas separation

There are still many challenges such as interface defects during the preparation of the MMMs. These defects can be the consequences of the weak polymer-sieve interaction and properties of the polymer and sieve phase. The gas separation performances of the MMMs can be affected negatively due to these defects. This is divided into three sections such as interface voids, pore blockage and chain rigidification. Firstly, incompatibility between polymer phase and filler can cause formation of interfacial voids that is called as sieve-in-a cage morphology. As a result of formation of interfacial voids, the permeability increases with decreasing selectivity. Secondly, the pore entrances of the porous filler can be clogged up due to polymer chains, solvent or contaminant, which is called as partial pore blockage. The selectivity can be increase with decreasing permeability when partial pore blockage occurs. Lastly, non-selective interfacial voids can form due to poor adhesion between filler material and polymer phase. Gas molecules pass through these nonselective voids during

the transportation because of its low resistance. Therefore, the selectivity decreases with increasing permeability [48, 86-88].

Recently, Mixed Matrix Membranes have been the subject of research because they have showed the potential for improved gas separation performance. However, the problem of interface defects between filler and polymer matrix is still under investigation. Many researchers are trying to improve the performance of MMMs by observing the effect of different parameters and using different approaches.

Ismail et al. [36] studied separation performances of the polyethersulfone/polyimide (PES/PI)/Zeolite-4A MMMs. The loading amounts of Zeolite-4A were varied between 10 and 50 wt % of the polymer. For mixed matrix membranes that were annealed above Tg, the permeability of O_2 decreased compared to below Tg annealed membranes. Also, the ideal O_2/N_2 selectivity was improved by a factor of 5 for the mixed matrix membranes which were annealed above Tg.

Süer et al. [88] studied the preparation method effects of polyethersulfone (PES)/ Zeolite 13X or 4A MMM with different amount of zeolite loadings. Permeability and selectivity values were improved at high loading amounts of Zeolites 13X and 4A (50 w%). However, permeabilities decreased in both PES/zeolite 13X and PES/Zeolite-4A MMM when zeolite loading increased. Permeabilities started to increase at certain amount of zeolite loadings which were above 8 wt % and 25 wt % for Zeolite-13X and Zeolite-4A, respectively. They concluded that the membrane morphology and gas separation performance was affected by zeolite type, significantly. Also, formation of microvoids and partial incompability between polymer matrix and zeolite were observed.

Another study, which related to the surface modification with silane coupling agents, was examined by Mahajan et al. [60]. Matrimid/Zeolite-4A MMM produced with modified and unmodified zeolites. When modified Zeolite-4A was used into the MMM, the selectivity of O_2/N_2 was the same as the O_2/N_2 selectivity of pure Matrimid membrane. However, both the permeability and selectivity were increased by using unmodified Zeolite-4A into the membranes. They concluded that the surface modification with silane coupling agents did not enhance the separation performances of the membranes due to unreduced non-selective voids in the polymer phase.

Bassem et. al [89], fabricated a pure Poly Ether Imide (PEI) membrane and 5 wt% nZIF-7/PEI MMM by solution casting technique and annealed it at 100°C for 18h. The thickness of the membranes was reported as 300μm. They tested the membranes for O_2 and N_2 permeabilities at feed pressure of 2 bar and a temperature of 35°C. The permeability and selectivity of PEI was reported as 120 barrers and 5.5. They found that the permeability and selectivity decreased with the introduction of nZIF-7 into PEI membrane as the MMM showed permeability of 16 barrers and selectivity of 4.2.

2.8. Physical Ageing

The free volume of glassy polymer membranes generally decreases with time. This process is called “Physical Ageing”. It usually results in decreased permeability with a slight increase in selectivity [90].

The effect of physical ageing on Matrimid polymer was examined by Ansaloni et.al [91] by performing the permeability tests (CO_2 and CH_4) for every 1000 hours up to 3000 hours. They found that permeability decreased by 25 % with no significant change in selectivity. The reason for this behavior was explained as the regaining or stabilizing of polymer structures configuration which changed after annealing at high temperatures.

To summarize literature review, it can be observed that the annealing temperature and time play an important role in increasing the gas separation performance of the pure polymer and MMM. Moreover, Matrimid-ZIF-8 MMM has been prepared and annealed only up to 240 °C. Hence MMMs can be prepared and annealed at higher temperatures, to achieve higher selectivity so that it can surpass Robeson upper bound curve. On the other hand, crystal size of ZIF-8 is also important in polymer-filler interface contact. It is observed that the smaller the crystal, the higher the surface area and hence better contact with Matrimid polymer. It can be inferred from literature that by using the stirring time of 5 min and excess of Methanol [Zn : Hmim: MeOH =1:4:1500], ZIF-8 with average crystal size of 20-30 nm can be achieved.

CHAPTER 3

EXPERIMENTAL

3.1. Synthesis of ZIF-8

Zinc Nitrate Hexahydrate [Zn $(NO_3)_2$. $6H_2O$, 99% purity], 2-Methyl Imidazole (2-MeIm, 99% purity), Methanol from LOBACHEMI were used to synthesize ZIF-8.

ZIF-8, was synthesized by using the molar ratio of Zn^{2+} : 2-methylimidazole : Methanol = 1 : 4 : 1500 prepared as the following method.

Zn $(NO_3)_2$. $6H_2O$ was dissolved in 50 ml of Methanol by stirring at 120 rpm using magnetic stirrer for 10 minutes (Solution 1). In parallel, 2-methylimidazole was dissolved in another 50 ml Methanol by stirring at 120 rpm using magnetic stirrer for 10 minutes (Solution 2). Solution 2 was mixed with Solution 1 and stirred for 5 minutes. The developed milky dispersion was kept settling for 1 day so that the ZIF-8 nanocrystals precipitate at the bottom of the flask. The ZIF-8 nanocrystals were separated from the colloidal dispersion by centrifugation at 5000 rpm for 1 hour. Washing with fresh Methanol followed by centrifuging at 5000 rpm for 30 minutes was repeated three times. The product was dried at 70 °C in an oven for 12 hours. The percent yield of ZIF-8 was calculated based on maximum amount of ZIF-8 that can be handled in the situation that all the Zn^{+2} source is consumed in the synthesis solution [Appendix A].

3.2. Membrane Preparation

3.2.1. Pure Matrimid Membrane Preparation

Matrimid membrane was prepared by solution casting and solvent evaporation technique. Chloroform ($CHCl_3$, 99% purity, from Sigma-Aldrich) was selected as solvent as it evaporates quickly at room temperature. Initially, Matrimid powder (from Alfa-Aesar) was vacuum dried at 120 °C for 12 hours to remove any entrapped moisture. 0.44g (10 wt%) of dried Matrimid were then dissolved in 4 g of Chloroform at room temperature by stirring at 120 rpm using magnetic stirrer for 1 hour. The viscous solution was then poured into a petri-dish and then it was covered with lid in Chloroform environment. After casting, the solvent slowly evaporates leaving a thin and uniform polymer film which was later (after 24 hours) peeled off. The thickness of the membrane was measured using micrometer and the average of measurements of 10 different locations points was recorded. .

3.2.2. Matrimid/ZIF-8 Mixed Matrix Membranes (MMMs) Preparation

Mixed Matrix Membranes (MMMs) were prepared by varying the loading of ZIF-8 (5, 10, 20, 30, and 40 wt%) in Matrimid polymer matrix. The weight loading of ZIF-8 in the nanocomposite membrane was defined as:

$$\boldsymbol{Wt_{ZIF-8}\,\%} = \left[\frac{\boldsymbol{m_{ZIF-8}}}{(\boldsymbol{m_{ZIF-8}} + \boldsymbol{m_{Matrimid}})}\right] \times \mathbf{100}$$

Mixed Matrix Membrane was in the following steps (Schematic for MMM dope solution preparation is shown in Fig. 15):

1) Initially, Matrimid powder and ZIF-8 nanocrystals were vacuum dried at 120 °C for 12 hours to remove any entrapped moisture.
2) 0.66g of dried Matrimid was then dissolved in 6g of Chloroform at room temperature by stirring at 120 rpm using magnetic stirrer for 60 minutes.
3) In parallel, calculated amount of ZIF-8 (each for 5, 10, 20, 30, 40 wt%) was uniformly dispersed in 4g of Chloroform by sonication using ultrasonic probe sonicator for 20 minutes.
4) Then, 15wt% (approx.) of the polymer solution was added to the ZIF-8 suspension and sonicated for 20 min (This process is called “priming” which is done to avoid particle agglomeration and to make sure that ZIF-8 particles have a coating of Matrimid polymer solution and no void formation take place).
5) Finally, the rest of the polymer solution was added to the above solution and sonicated for 60 minutes resulting in the formation of MMM solution.
6) The viscous solution was then poured into a petri-dish and then it was covered with lid in Chloroform environment.
7) After casting, the solution was left to settle for 24 hours, so that the solvent evaporates leaving a thin and uniform polymer film.
8) The film was then vacuum annealed at temperature where Matrimid shows optimum gas separation properties to get enhanced O_2/N_2 gas separation performance.

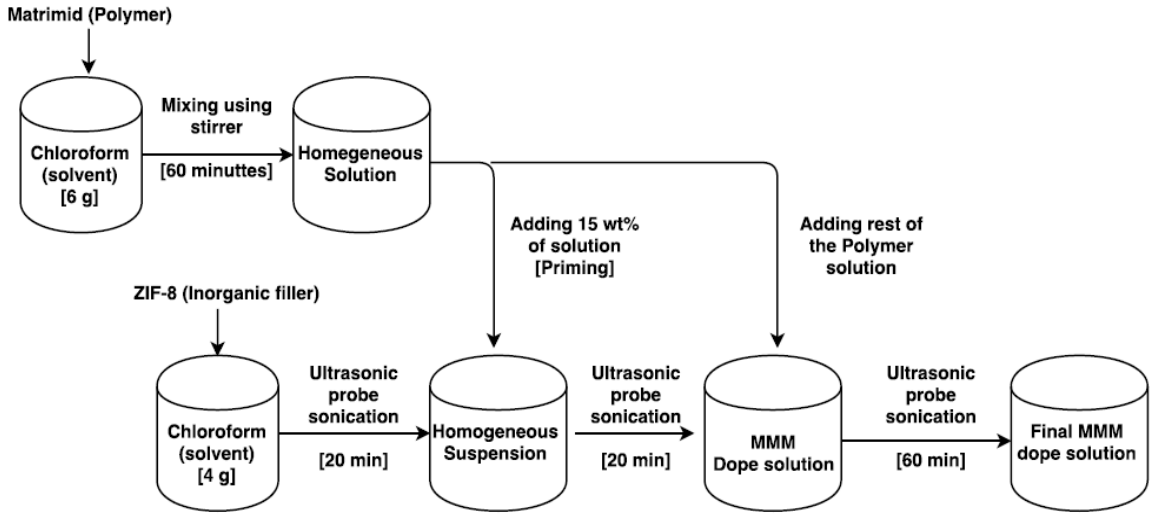

Figure 15: Schematic showing MMM dope solution preparation method

3.3. Thermal Annealing

Matrimid membranes were thermally annealed in vacuum environment in a tube furnace equipped with temperature controller which was sealed on both ends (Fig. 16) and the temperature was measured using thermocouple. The heating rate used was maintained constant at 2°/min throughout the experiments.

Initially, the membranes were cut into circular shape of 1 inch diameter and put in furnace for annealing at 80,120, 250 and 300 °C respectively for 12 hours. It was observed that there was no change in diameter for membranes heated up to 300 °C but the Matrimid membrane was found to shrink above 300 °C. The shrinkage for 320 °C, was measured to be 10%.

To find the effect of Time on O_2/N_2 gas separation performance, annealing was done by varying time durations (1, 12, 24, 36 hrs.) at the optimum temperature.

Figure 16: Tube Furnace for Thermal Annealing of Matrimid and MMMs

When the optimum annealing temperature and time for enhanced O_2/N_2 gas separation performance was found, MMMs (5, 10, 20, 30 and 40 wt %) were also thermally annealed in vacuum at this optimum annealing temperature and time.

3.4. Characterization

The theoretical densities of Matrimid polymer (ρ_p) and ZIF-8 filler (ρ_f) are 1.2 g cm^{-3} and 0.95 g cm^{-3} [35, 64], respectively. Based on these densities and the mass of Matrimid (m_p) and ZIF-8 (m_f) used, the theoretical densities of the MMM was calculated using the Eqn. 7.

$$\boldsymbol{\rho_{MMM}} = \frac{\mathbf{m_p + m_f}}{\mathbf{m_f/\rho_f + m_p/\rho_p}} \qquad (7)$$

The volume fraction of ZIF-8 (φ) in Mixed Matrix Membranes (MMMs) can be calculated by the Eqn. 8.

$$\boldsymbol{\varphi_D} = \frac{\mathbf{m_f/\rho_f}}{\mathbf{m_f/\rho_f + m_p/\rho_p}} \qquad (8)$$

3.4.1. Scanning Electron Microscope (SEM)

SEM analysis was carried out to study the morphology and crystal structure of ZIF-8, Pure Matrimid structure, and the distribution of ZIF-8 crystals in Matrimid/ZIF-8 MMMs.

Sample preparation for ZIF-8 was done by using a small quantity of ZIF-8 particles and a Copper conductive tape which is double sided adhesive. One side of the tape was applied on SEM sample holder and the on other side ZIF-8 particles were spread and then coated using Gold sputtering instrument (Ion Sputter JFC-1100) to reduce the charging effects. Similarly, the cross-sectional samples of Matrimid and MMMs were prepared for SEM analysis by freeze fracture [25, 64] after immersing in Liquid Nitrogen for 5-10 minutes and subsequent gold layer coating. Then Secondary Electron Images were taken using SEM (JEOL: JSM-6460LV) at accelerating voltages of 5 kV and 10 kV.

3.4.2. X-ray Diffraction

X-ray Diffraction Analysis for the synthesized ZIF-8 nanocrystals was performed using Bruker X-ray diffractometer (XRD) With Cu-Kα radiation in the 2θ angle ranging from 2° to 40° at a step increment of 0.02°/sec. The voltage and current used were 30 kV and 30 mA, respectively. The crystal size was also calculated using the following Scherrer equation (Eqn. 9) corresponding to the highest intensity peaks.

$$\textbf{Crystal size, L} = \frac{\mathbf{k}*\boldsymbol{\lambda}}{\mathbf{FWHM}*\mathbf{Cos}\boldsymbol{\theta}} \qquad \textbf{(9)}$$

Where, k (shape factor) = 0.94, λ= 0.154 nm, FWHM = Full Width Half Maximum (radians)

3.4.3. Thermo-Gravimetric Analysis (TGA) and Differential Scanning Calorimetry (DSC)

SDT Q 600 V20.9 instrument which features highly reliable horizontal dual balance mechanism and supports both TGA and DSC measurements simultaneously was used to determine the thermal stability of the ZIF-8 nanocrystals in inert N_2 environments.

A small quantity (approx. 5 mg) of synthesized ZIF-8 nanocrystals were placed in alumina pans and the samples were heated from 25°C to 800°C at a heating rate of 5°C /min in Nitrogen environment (gas flow rate of 50 ml/min). TGA analysis was done by plotting Weight loss Versus Temperature graph.

The glass transition phase of Matrimid was studied by carrying out DSC experiment. A 5mg of Matrimid powder was placed in alumina pan and the sample was heated from 25 ^oC to 380^oC at a heating rate of 10^oC/min. The Heat flow Versus Temperature graph was used to find the glass transition temperature.

3.4.4. Nitrogen Adsorption – Desorption analysis

To find the surface area and pore size of ZIF-8 nano-crystals, N_2 adsorption – desorption analysis was carried out at 77 K using Quantachrome Instruments (V 6.0).

A 85 mg sample of ZIF-8 was initially degassed for 6 hours under high vacuum and then placed in QuadraSorb Station 1 for N_2 adsorption-desorption analysis. The specific surface area (S_{area}) of ZIF-8 was calculated using Brunauer - Emmett - Teller (BET) Model while the pore size and volume was evaluated from the non-linear Density Functional Theory (DFT) model.

3.5. Gas Permeability Set-Up and Procedure

3.5.1. Gas permeability Set-up

The gas permeation experiments were conducted in a constant-volume variable-pressure system to be used for single gas experiments which was built according to the literature present elsewhere. The schematic drawing of the experimental set-up is shown in Fig. 17. It consists of a membrane cell, a single wall pressure controller (Alicat Scientific Inc.), a digital pressure gauge (Alicat Scientific Inc.), gas cylinders (O_2 and N_2), a vacuum pump, a vacuum reservoir.

The membrane cell has a filter paper and stainless steel sieve whose purpose is to support the film or membranes that has to be tested. The membrane has to be placed in this cell and covered with double-Viton O-ring seals which prevents the air leakage. A single valve **pressure controller gauge** is used at the feed side, which serves for 2 purposes, it can read as well as control the pressure (up to a set point) while a digital **Pressure gauge** is used at the permeate side which records the downstream pressure rise. These two pressure gauges are connected to a data acquisition system through USB ports which is connected to a computer. The data of feed pressure and permeate pressure rise with time was recorded using FLOW VISION software, at sampling rate of 1 record / sec. The operating temperature and feed pressure were 23ºC and 7 bar, respectively. The dead volume of the set-up was measured as 0.5 cm^3 which is the volume from permeate side of the membrane cell to the pressure transducer. The effective area of the membrane through which gas actually passes was calculated as 2.54 cm^2.

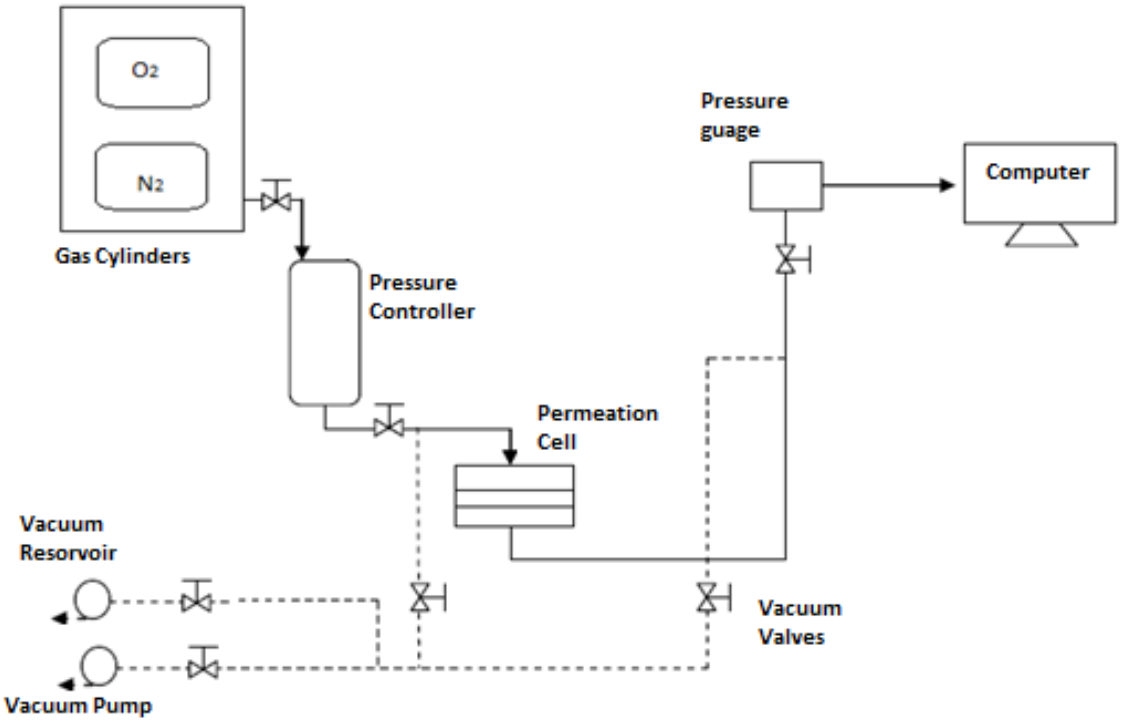

Figure 17: Schematic of single gas permeation experimental setup

3.5.2. Permeability experiment procedure (Time-lag Analysis)

For each experiment, circular shaped membranes of 1 inch Diameter has to be inserted into stainless steel cell and both sides of the membrane have to be evacuated for 1 hour using vacuum pump to remove any gas present in the film. Then the gas has to be fed from the feed side at a pressure of 7 bar and the downstream pressure rise against time was recorded to calculate permeability. The variation of Upstream pressure (feed pressure) and downstream pressure (permeate side) along with the time were recorded [using flow vision software] to calculate the raw slope dp/dt [92, 93]. Leakage was calculated for O_2 and N_2 by recording the slope of permeate pressure rise Versus time plot for placing impermeable membrane in permeation cell and feeding the corresponding gas at a pressure of 7 bar

(operating condition). This leakage was subtracted from the "raw slope" to get the "corrected slope" which is substituted in the formula of permeability in Eqn. (11)

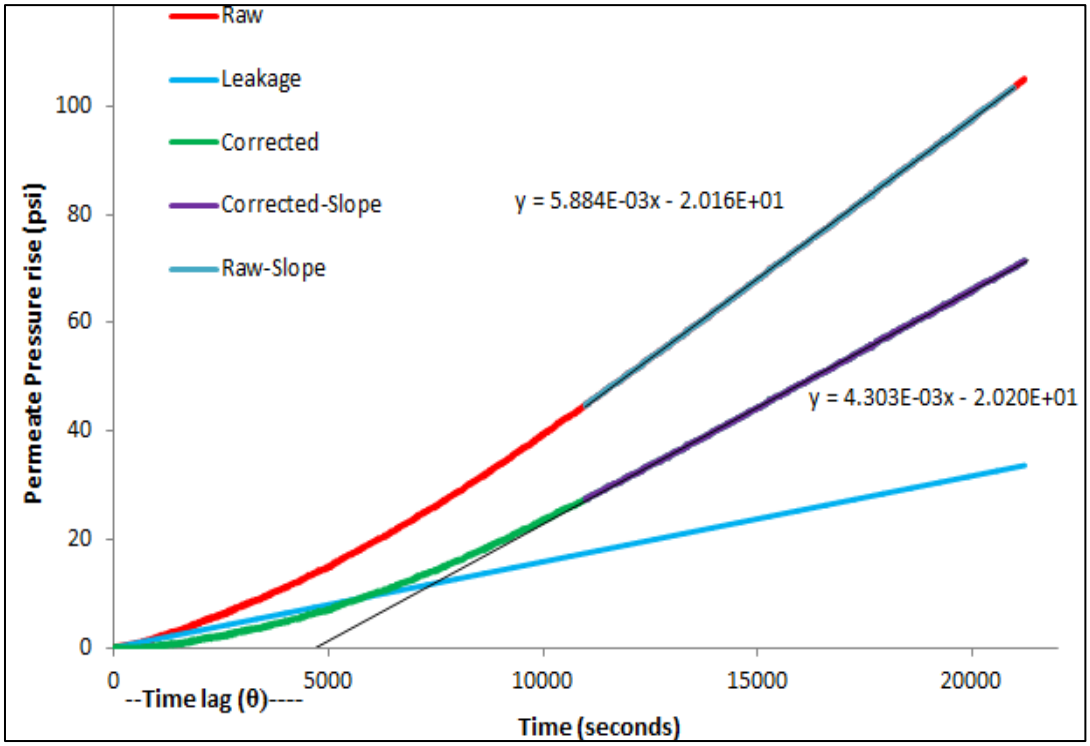

Figure 18: Schematic showing Time-lag analysis for N_2

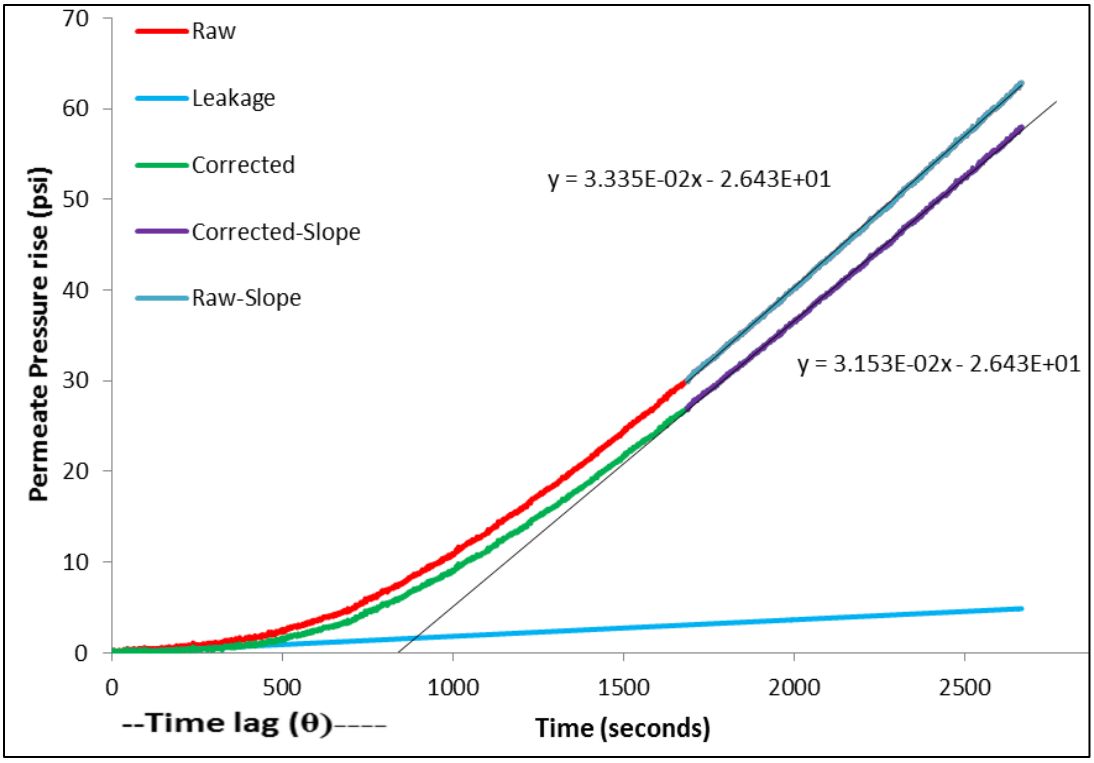

Figure 19: Schematic showing Time lag analysis for O_2

According to the time lag method, the Time-lag (θ) is calculated as X-intercept of the Pressure rise Versus Time plot as shown in the figure 18 and 19.

$$\mathbf{D = L^2/6\theta} \qquad \textbf{(10)}$$

$$\mathbf{P = 22414 * 10^{10} * \frac{V}{RTA} * \frac{L}{p1-p2} * \frac{dp}{dt}} \qquad \textbf{(11)}$$

Where,

V = Volume = 0.5 cm^3, R = Gas constant = 6236.56 cm^3.cmHg / mol·K,

T = Temperature = 23°C, A = Effective area = 2.54 cm^2, L = Membrane thickness (cm),

p1= feed side pressure = 7 bar, p2 = permeate side pressure = 0,

dp/dt = slope calculated from the experiment (Permeate pressure rise Versus Time plot).

$$\text{We know that,} \quad \mathbf{P = S * D} \qquad \mathbf{(12)}$$

$$\text{Hence,} \quad \mathbf{S = P/D} \qquad \mathbf{(13)}$$

The recording time interval changes from gas to gas according to the duration of permeation tests which depends on the gas and the membrane. Diffusivity (D) and Solubility (S) coefficients are calculated by the Equations (10) and (13).

CHAPTER 4

RESULTS AND DISCUSSIONS

The experimental approach is shown in Fig. 20. In the present study, ZIF-8 nanocrystals were synthesized at room temperature with minimum crystal size to have improved compatibility between the ZIF-8 and polymer and to avoid interfacial defects. Pure Matrimid membranes were prepared by solution casting technique and the effect of annealing temperature and time on O_2/N_2 gas separation performance was studied.

Mixed Matrix Membranes (MMMs) were prepared by varying the amount of ZIF-8 (5-40 wt%) in Matrimid polymer and annealed under vacuum at the optimum temperature and time. The effect of chemical treatment on O_2/N_2 gas separation performance of MMMs was also studied by treating MMM - 40 wt% membrane with Ethanol and Ethylene Glycol. The fabricated Matrimid and MMMs were characterized using SEM, XRD, TGA and DSC to understand its morphology, crystal structure, thermal properties and to inspect the polymer and ZIF-8 interface.

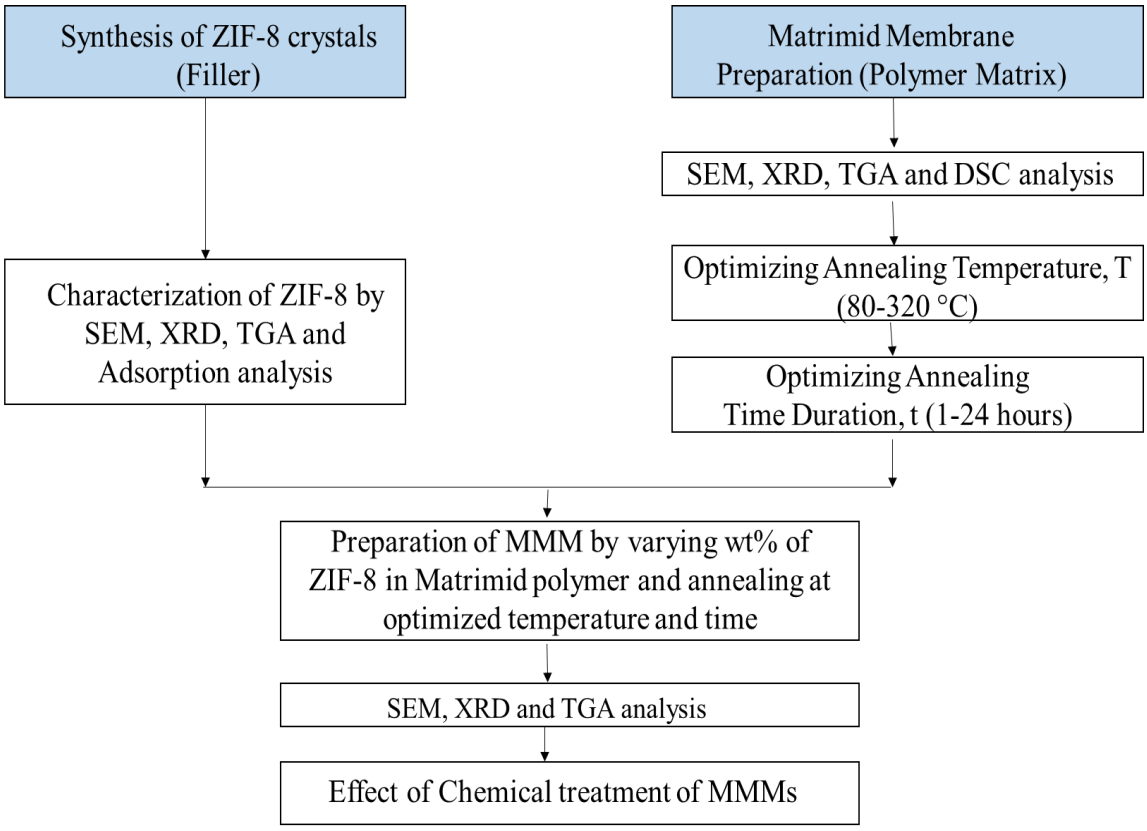

Figure 20: Flow Chart showing the experimental approach

Pure matrimid membranes were prepared and annealed at various temperatures and time durations. They were tested for permeability of O_2 and N_2 respectively. The effect of annealing temperature and time on O_2/N_2 Gas separation performance of pure Matrimid is discussed in this chapter. Then, MMMs were prepared by varying the content of ZIF-8 in pure Matrimid polymer and annealed at optimum temperature and time. Their effect on O_2/N_2 Gas separation performance is also discussed.

The bulk density of pure Matrimid and Mixed Matrix Membranes were estimated by their ratio of Area and Volume. They are reported in Table 3. It can also be observed that bulk density of MMMs is usually less than the theoretical value owing to the formation of voids.

Table 3: Densities of Pure Matrimid and MMMs, annealed at 320°C for 12h

S. No	Membrane	ZIF8 wt%	Mass of Matrimid (m_C),g	Mass of ZIF8 (m_D), g	Vol. Fraction of ZIF-8, φ	Theoretical Density, ρ_t	Estimated Density, ρ_B
1	**MMM - 5wt%**	5	0.66	0.035	6.2%	1.18	1.18
2	**MMM - 10wt%**	10	0.66	0.073	12.3%	1.17	1.12
3	**MMM - 20wt%**	20	0.66	0.165	24.0%	1.14	1.04
4	**MMM - 30wt%**	30	0.66	0.283	35.1%	1.11	0.92
5	**MMM - 40wt%**	40	0.66	0.440	45.7%	1.09	0.86

4.1. Effect of Annealing Temperature on O_2 and N_2 Gas Permeability of Pure Matrimid

The effect of annealing temperature on permeability and selectivity of pure Matrimid was studied by annealing Matrimid membranes at 80, 120, 250, 300 and 320 °C under vacuum for 12 h. Permeability test of the prepared films for O_2 and N_2 gases was done at feed pressure of 7 bar and room temperature (23 °C) and the results are summarized in the Table 4 and Fig. 21.

Table 4: Permeability test results for Matrimid annealed at different temperatures (Time constant at 12 hours)

Annealing temp (°C)	Permeability (O_2), Barrers	Selectivity (O_2/N_2)	Diffusivity [$\times 10^{-8}$ cm^2/sec]		Solubility [$\times 10^{-3}$ $cm^3(STP)$ cm^{-3} $cmHg^{-1}$]	
			O_2	N_2	O_2	N_2
80	**0.79**	**5.46**	2.91	2.41	2.73	0.60
120	**0.45**	**6.44**	1.12	0.36	4.04	2.01
250	**0.43**	**8.76**	0.76	0.28	5.76	1.78
300	**0.38**	**11.75**	1.38	0.78	2.76	0.42
320	**0.36**	**15.87**	1.36	0.42	2.69	0.55

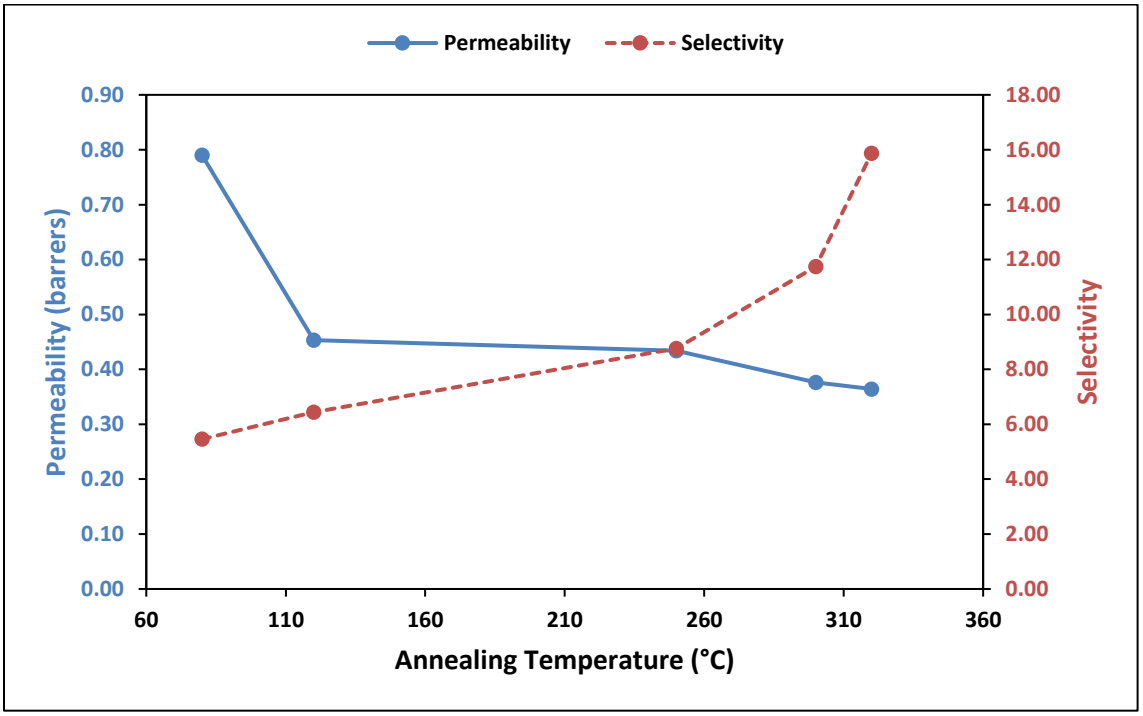

Figure 21: Effect of Annealing temperature on Permeability and Selectivity (Time constant at 12 hours)

It can be observed from Fig. 21, that as the annealing temperature increases from 80°C to 320°C, the selectivity of polymer increased significantly from 5.46 to 15.87 with a simultaneous decrease of permeability from 0.79 to 0.36 barrers. The permeability dropped significantly from 0.79 to 0.45 barrers with increase in annealing temperature from 80°C to 120°C because the entrapped Chloroform solvent is removed. The reason for this is due to the boiling point of chloroform being 62°C, and heating the membrane for 12 hours at 120°C would drive out all the chloroform.

As the annealing temperature increases, it promotes the thermal motion and rearrangement of the polymer chains which may result in formation of Charge Transfer Complexes (CTCs) [94-96]. CTCs are weak, intra- and inter-molecular, bonds between the electron-

rich Aromatic ring and the electron-deficient Imide ring of the Matrimid, formed by the donation of π-electrons as shown in Fig. 22 [63]. This behavior increases the packing density of the polymer chains and decreases the free volume [63, 97]. As a consequence, the membrane annealed at higher temperature may have a smaller free volume, resulting in high selectivity and low permeability. CTC formation is usually not accompanied with chemical reactions or modifications of the chemical structure of the polymer molecules. FTIR analyses of all samples, annealed at different temperatures, are shown in Fig. 23. The results clearly show that there are no changes in peaks/bands with increase in temperature. Hence, it can be concluded that CTCs might have been formed as the annealing temperature was increased from 80 to 320°C.

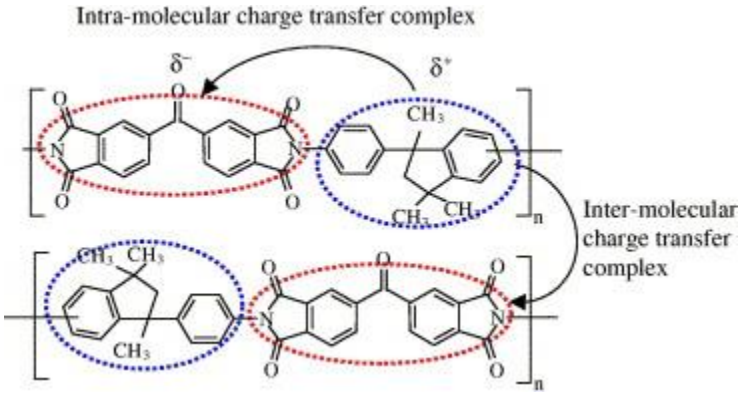

Figure 22: Schematic showing Inter and Intra CTC formation

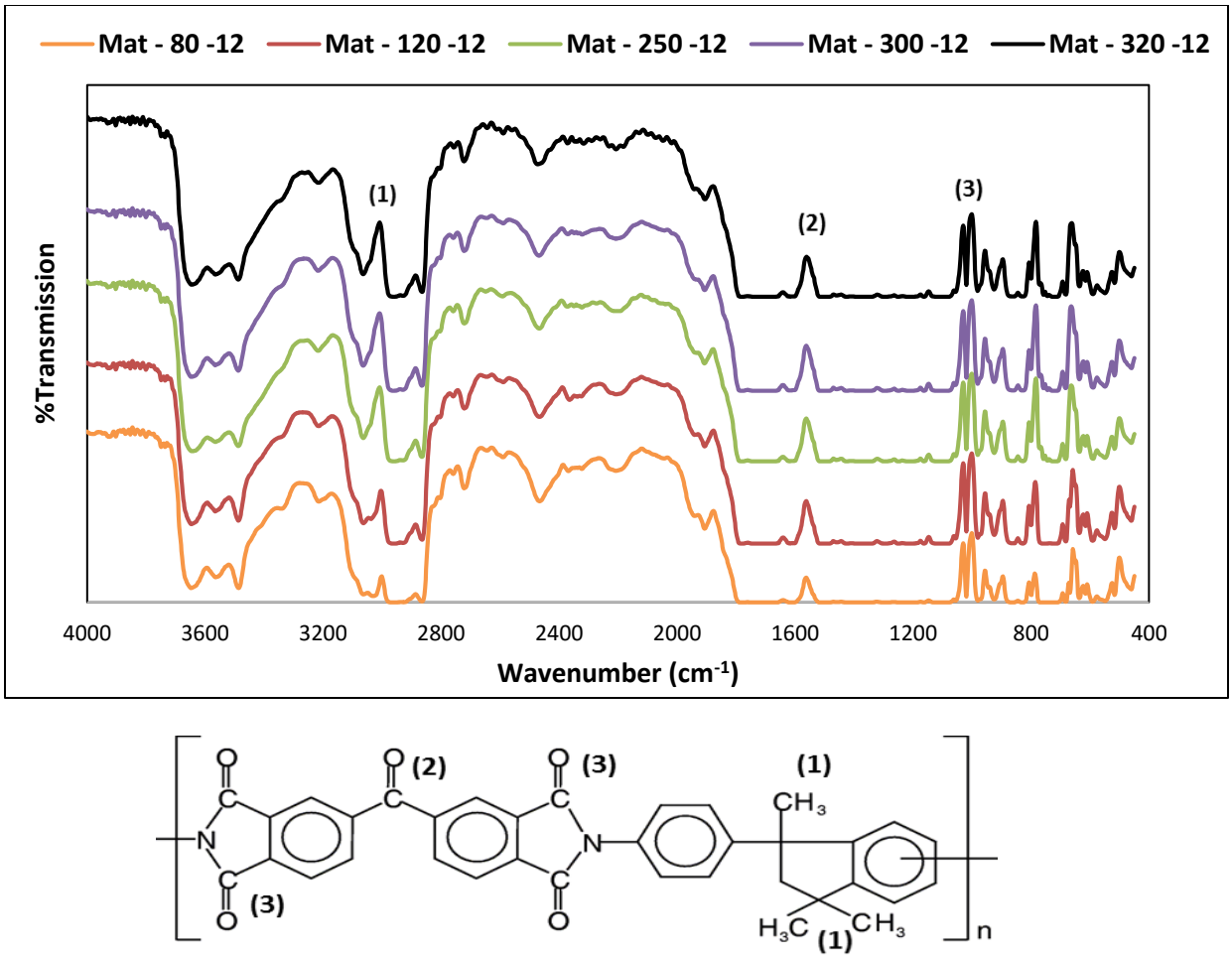

Figure 23: FTIR results for Matrimid membranes annealed at 80-320°C for 12 h

Barsema et.al. [63] found that annealing Matrimid above Glass transition temperature, Tg results in formation of Charge transfer Complexes (CTCs) while annealing below Tg results only in structural densification of polymer chains. Hence, to analyze further, Tg of pure Matrimid powder was found by carrying out DSC analysis.

Differential Scanning Calorimetry (DSC) plot of Matrimid is shown in Fig. 24 which clearly shows 280-320°C is the glass transition phase region, which is also in accordance

with the Literature [98]. But, Matrimid annealed at 320 °C for 12 h doesn't form CTC and its high selectivity (15.87) is mainly due to polymer chain densification.

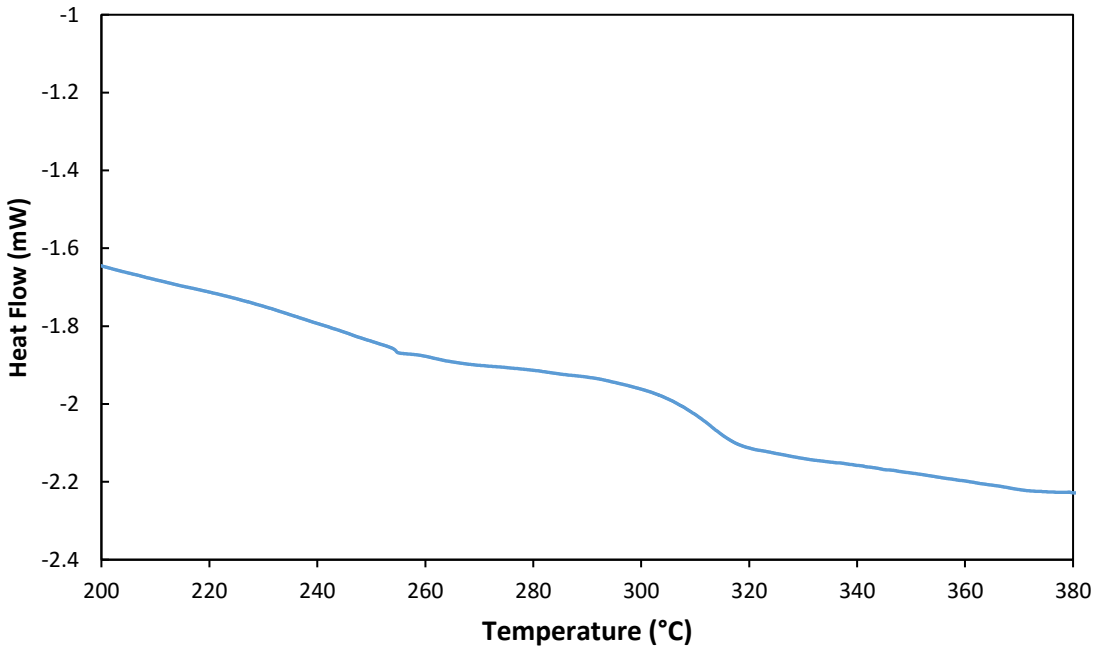

Figure 24: DSC plot of Pure Matrimid

The optimum O_2/N_2 gas separation properties were attained at 320 °C (Permeability =0.36 barrers and selectivity = 15.87) as the high selectivity is achieved at this temperature. The Matrimid membrane was also subjected to annealing at 330 °C for 12 hours to carry out the study further, but the membrane became too brittle to be tested for permeability.

4.2. Effect of Annealing Time on O_2 and N_2 Gas Permeability of Pure Matrimid

The effect of annealing time on permeability and selectivity of O_2 was studied by annealing pure Matrimid membranes under vacuum at optimum temperature of 320 °C for 1, 12, 24,

and 36 hours. Permeability test of the prepared films for O_2 and N_2 gases was done at feed pressure of 7 bar and room temperature (23 °C) and the results are summarized in the Table 5 and Fig. 26. The diffusivity and solubility coefficients were also calculated and reported in Table 5. Matrimid membrane annealed at 320 °C for 36 hours showed low permeability for O_2 (0.05 barrers) and N_2 was expected to have still lesser permeability. Consequently, good time lag curve for N_2 was not obtained and hence it's permeability couldn't be determined.

The membranes changed their color from pale yellow to black as the annealing time varied from 1 h to 36 h as shown in Fig. 25.

Figure 25: Matrimid membranes annealed at 320°C for 1, 12, 24 and 36 h respectively.

Table 5: Permeability test results for Matrimid annealed at different annealing time durations (Temperature constant at 320 °C)

Annealing time (hrs)	Permeability (O_2) , Barrers	Selectivity (O_2/N_2)	Diffusivity [10^{-8} * cm^2/sec]		Solubility [10^{-3} * cm^3(STP) cm^{-3} $cmHg^{-1}$]	
			O_2	N_2	O_2	N_2
1	**0.38**	**9.48**	1.64	0.63	2.30	0.63
12	**0.36**	**15.87**	1.36	0.42	2.69	0.55
24	**0.23**	**20.69**	0.72	0.66	3.24	0.70
36	**0.05**	-	0.29	-	1.59	-

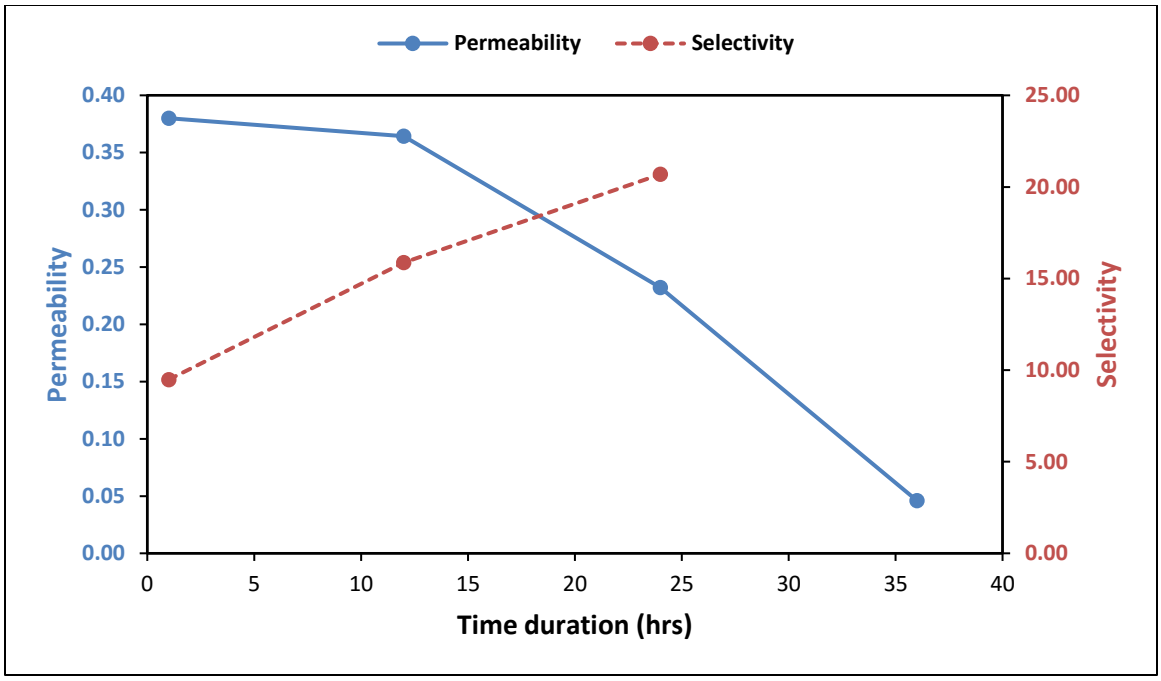

Figure 26: Effect of annealing time on permeability and selectivity at 320°C.

As the annealing time duration was varied from 1 to 24 hours at 320 °C, selectivity was significantly increased from 9.48 to 20.69 (118%), while permeability decreased from 0.38 to 0.23 barrers.

This significant increase of selectivity and decrease of permeability are due to chemical modification of the polymer molecules as illustrated by FTIR results (Fig.27). Even though the FTIR spectrum was saturated due to the membrane opacity, there is a clear variation of the peak intensity in the range of 3150 to 3300 cm^{-1}.

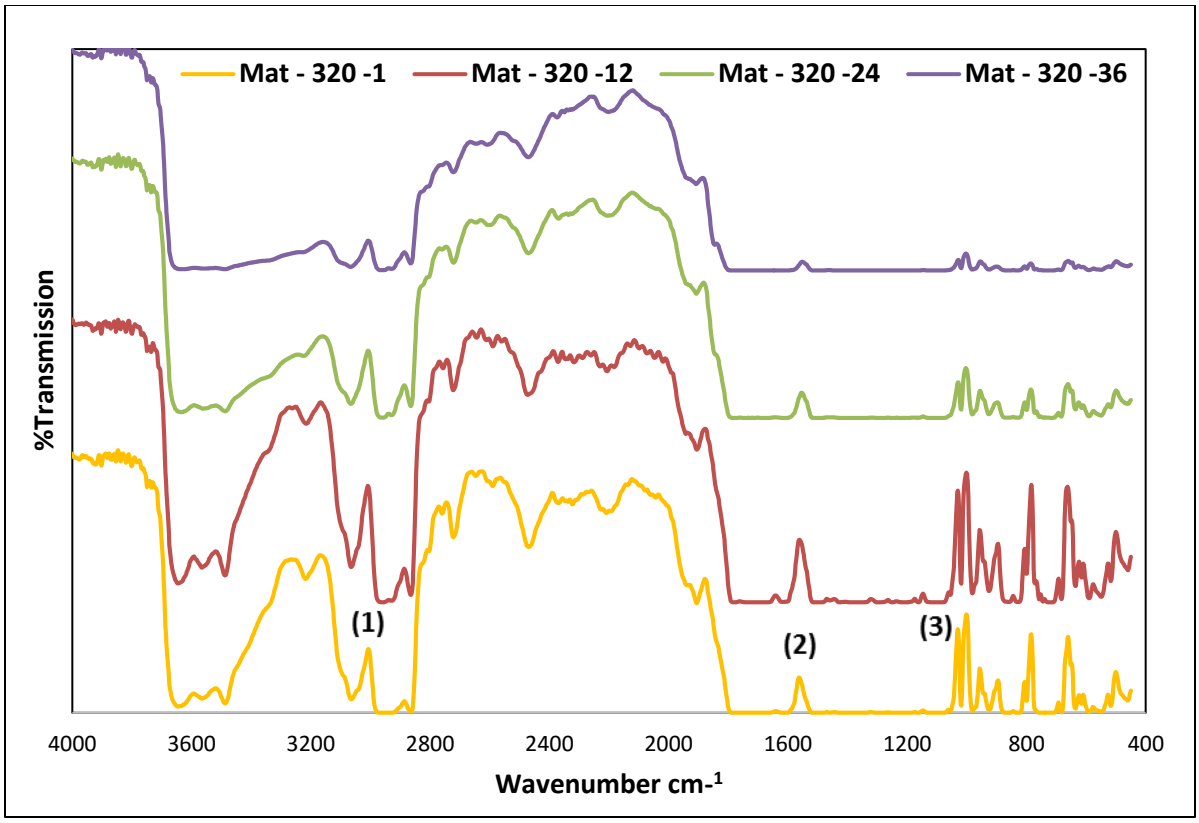

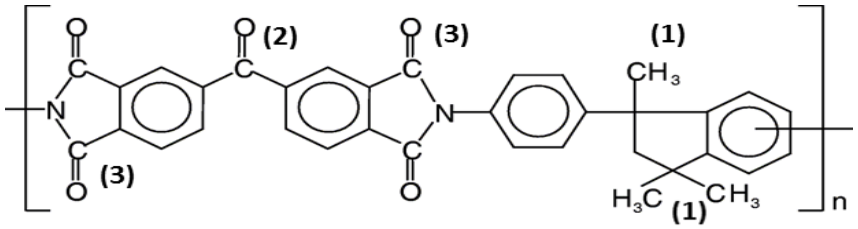

Figure 27: FTIR results for Matrimid annealed at 320°C for 1-36h

The permeability test results of Matrimid membranes annealed at different temperatures and time were plotted on Robeson chart of permeability versus selectivity as shown in Fig. 28. It can be clearly observed that two results surpassed Robeson present upper bound (2008), Matrimid annealed at 320 °C for 12 h and 24 h. respectively. But, they don't fall in the commercially attractive region as their permeabilities are too low (0.36 and 0.23 barrers).

Hence, to increase their permeabilities, ZIF-8 (which is known to have high permeability) nanocrystals have to be mixed with Matrimid membrane to form Mixed Matrix Membranes (MMMs) and annealed at optimum temperature (320 °C) and time. For this purpose i.e., to increase permeability of MMM to at least 1 barrer (so that it falls in the commercially attractive region [62]), 12 hours was selected as optimum time for annealing MMM because Matrimid shows high permeability at 12 hours (0.36 barrers) compared to that of 24 hours (0.23 barrers), making it easier to surpass Robeson upper bound and to achieve the minimum required permeability of 1 barrer.

Therefore, it can be concluded that the optimum annealing temperature and time for better O_2/N_2 gas separation performance were 320 °C and 12 h, respectively. Subsequently, all MMMs were annealed at this temperature and time.

The error analysis was done for the optimum temperature and time (320 °C, 12 h) by reproducing three Matrimid membranes followed by annealing them in vacuum at 320°C for 12 hrs. The membranes were then tested for permeability of O_2 and N_2 and the average value of permeability of O_2 was found to be 0.34 ± 0.025 barrers and selectivity was 16.46 ± 1.40. The corresponding error bars are also shown in Fig. 28.

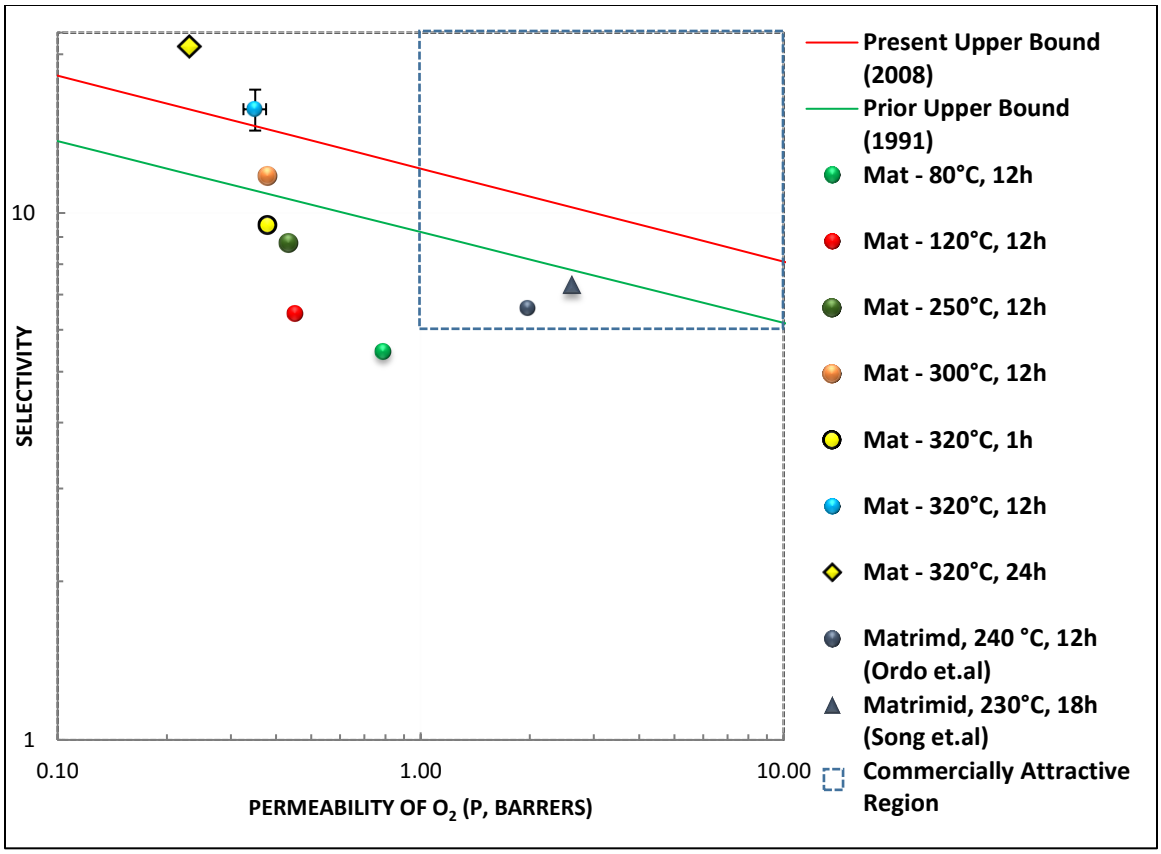

Figure 28: Permeability test results of Matrimid membrane on Robeson plot

4.3. ZIF-8 Loading Effect on O_2 and N_2 Gas Permeability of MMMs

ZIF-8 nanocrystals were synthesized and their crystal structures and sizes were determined using the XRD. Fig. 29 shows the XRD peaks and miller indices of the synthesized ZIF-8. The initial peak of (011) was found at $2\theta = 7.92°$ which is in accordance with literature of ZIF-8 [74]. The crystal size was calculated using Scherrer equation (Eqn. 14) corresponding to the peaks with high intensities i.e., (011), (112) and tabulated in the Table. 6. Their average value was calculated as 29.79 ± 0.065 nm.

$$D = \frac{k*\lambda}{FWHM*cos\theta} \qquad (14)$$

Where, D = Crystal diameter (nm); λ = wavelength of X-ray = 0.1542 nm;

θ = Bragg's diffraction angle; K = Scherrer constant = 0.94;

FWHM = Full Width at Half Maximum of the peak

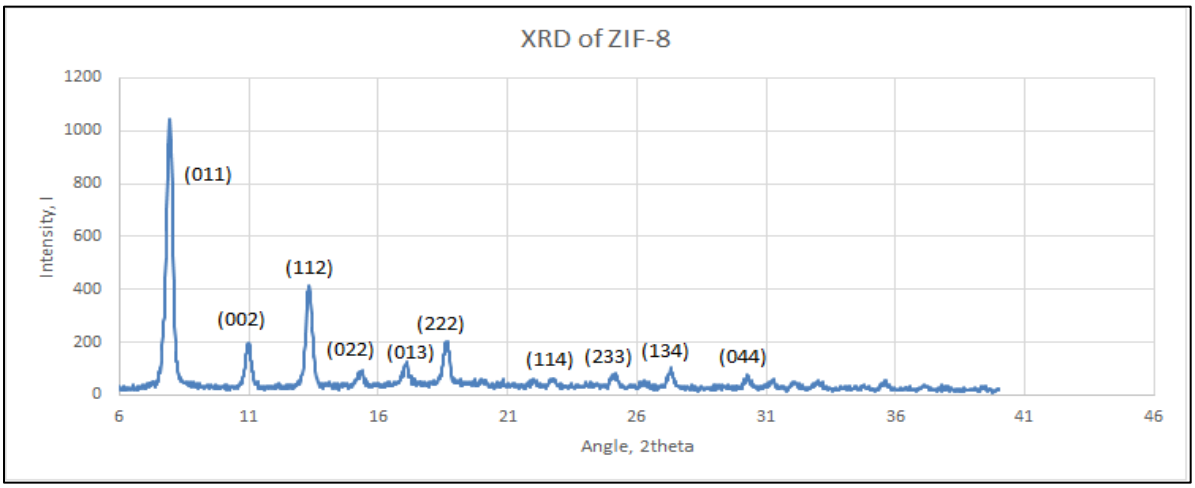

Figure 29: XRD pattern showing peaks and miller indices for ZIF-8 nanocrystals

Table 6: Crystal size corresponding to the peaks calculated using Scherrer equation

S.No.	Peak	Angle (2θ)	FWHM (°)	Crystal size (D, nm)
1	(011)	7.92	0.28	29.73
2	(112)	13.34	0.28	29.86
		Avg. crystal size (nm)		**29.79 ± 0.065**

Thermo-Gravimetric Analysis (TGA) was then done on the synthesized ZIF-8 nanocrystals in inert Nitrogen atmosphere to get the information of their thermal stability. The TGA plot of ZIF-8 nanocrystals is shown in Fig. 30. For the temperatures in the range of 20 to 350 °C, there was a slight decrease in the mass (<5 %) which relates to the removal of guest molecules (Methanol) from the cavities or unreacted 2-Methylimidazole from the surface of ZIF-8. From the temperatures, 350 -600 °C, there was a gradual decrease in the weight loss up to 20% which indicates beginning of thermal decomposition of ZIF-8.

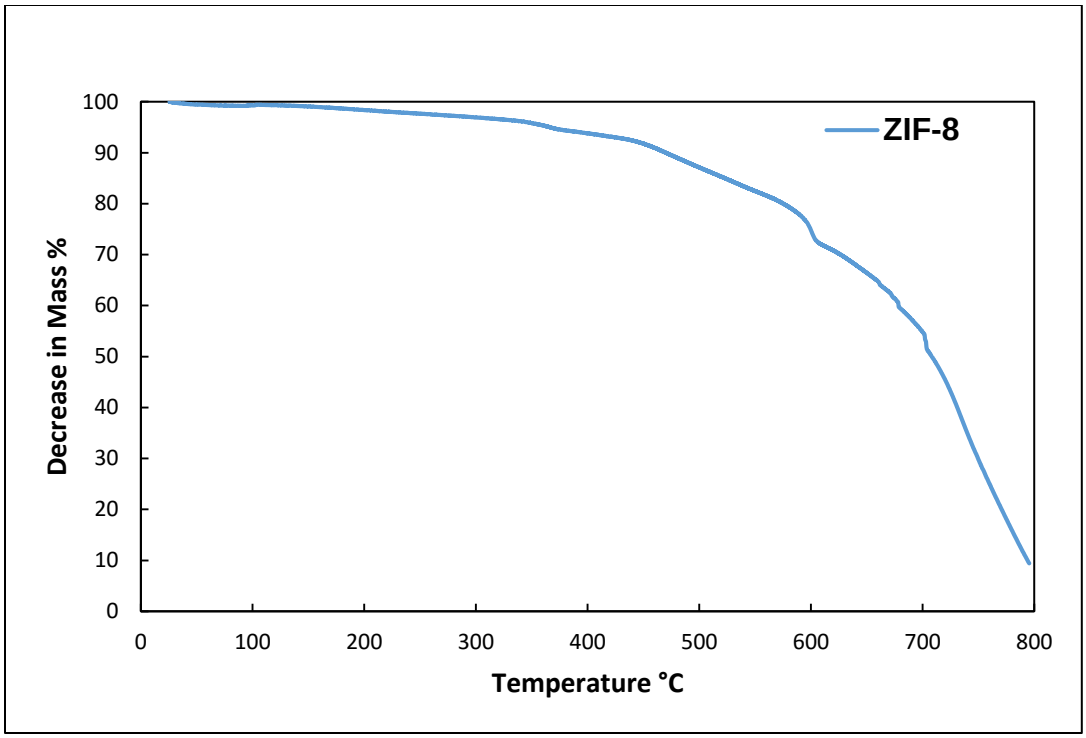

Figure 30: TGA plot of ZIF-8 nanocrystals

In order to find the pore size and surface area of the synthesized ZIF-8 nanocrystals, N_2 Adsorption-Desorption analysis was performed in inert atmosphere. The Nitrogen adsorption – desorption isotherms of ZIF-8 nanocrystals are shown in Fig. 31. The specific surface area (S_{area}) as calculated from BET model was found to be 1343 m^2/g which is in accordance with literature value of 1300 m^2/g [25]. Moreover, the pore size of ZIF-8 as estimated from non-linear Density Functional Theory (DFT) model was 5.88 A^o which is in consistent with pore size (5.8 A^o) of sodalite cage in ZIF-8 [35]. Fig. 32 shows the 3-Dimensional structure of ZIF-8 indicating its pore diameter (11.6 A^o). The pore volume was also estimated by the DFT model as 0.6478 cc/g which is also close to the literature value of 0.663 cc/g [35].

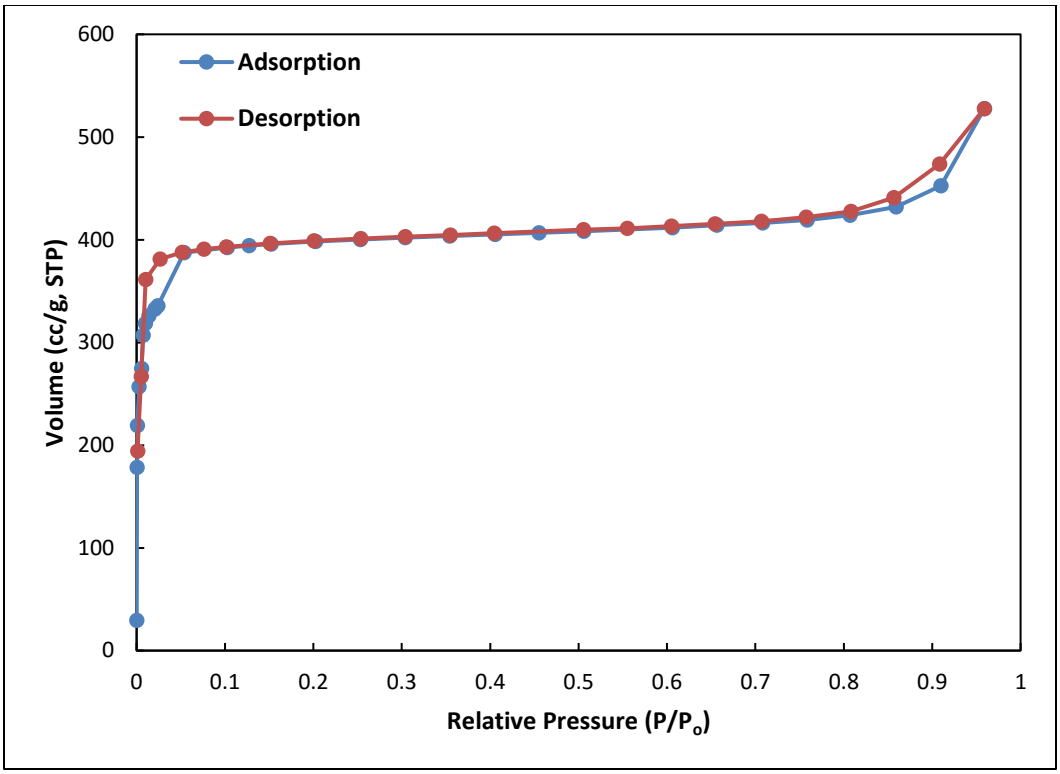

Figure 31: N_2 adsorption - desorption isotherms of ZIF-8

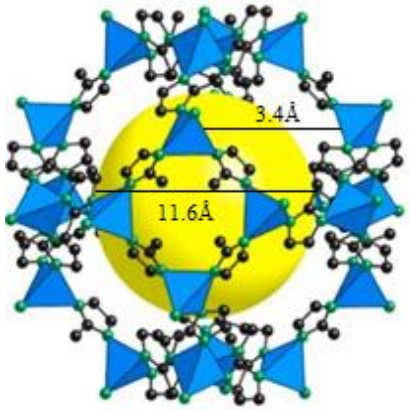

Figure 32: 3-D structure of ZIF-8 in cubic unit cell, showing large cavity (sphere region) with size 11.6Å and small apertures (six-membered ring window) with size 3.4Å [35]

MMMs were prepared by varying loading of ZIF-8 between 5 and 40 wt% in Matrimid polymer matrix. MMMs were then annealed under vacuum at the optimum temperature

and time of 320 °C and 12 hrs, respectively. To study the formation of membrane and interfacial contact, the Cross-sectional SEM analysis of MMMs and pure Matrimid was done. The surface shape and morphology of ZIF-8 was also studied using SEM.

Cross-sectional SEM image of Pure Matrimid as shown in Fig. 33 (a) shows a smooth, uniform dense Matrimid membrane. The SEM images of as synthesized ZIF-8 nanocrystals were taken at 10 kV accelerating voltage and at magnification of 63kX. It can be observed from Fig. 33 (b) the spherical shaped ZIF-8 crystals are formed. Fig 33 (c-f) shows the presence of honeycomb type of cavity network in MMM and the presence of voids which contribute to the permeability of MMM. It is clear that voids increase with increasing the content of ZIF-8. Moreover, MMMs doesn't show any sign of agglomeration of ZIF-8 nanocrystals which is very important. The MMMs fabricated by Ordonez et.al also showed similar SEM images [25].

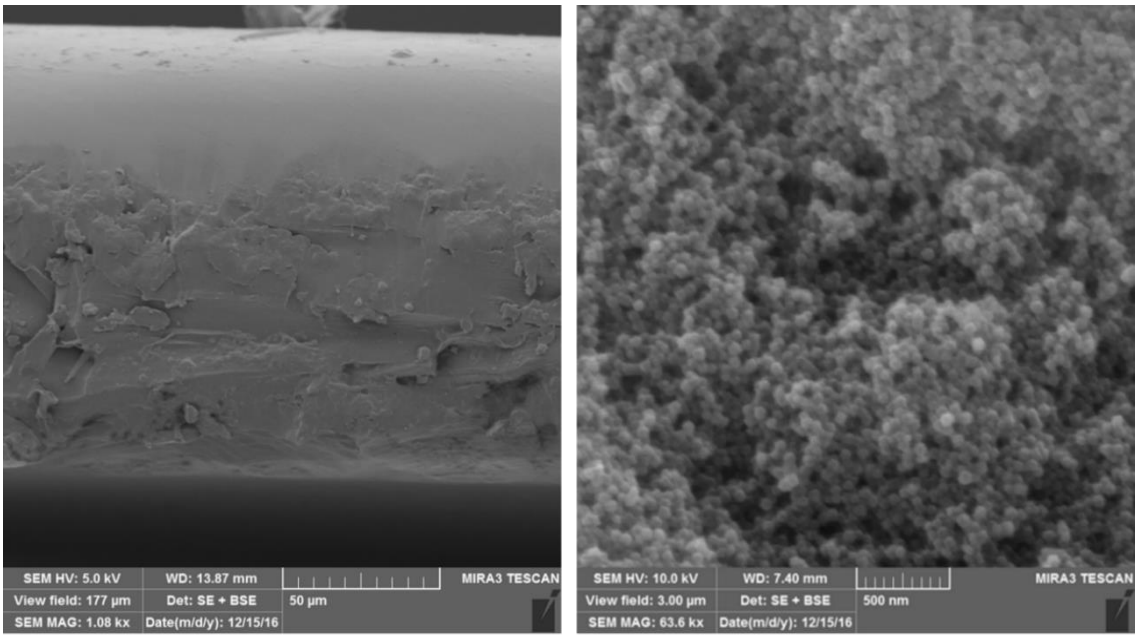

(a) Pure Matrimid (b) ZIF - 8

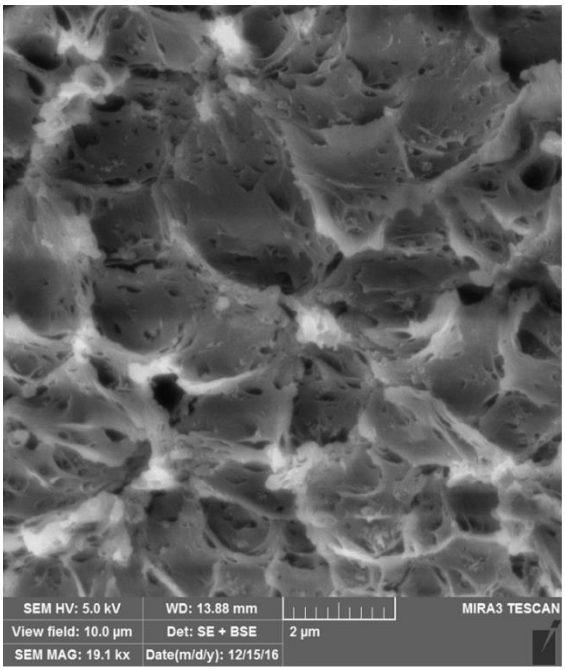

(c) MMM – 5 wt %

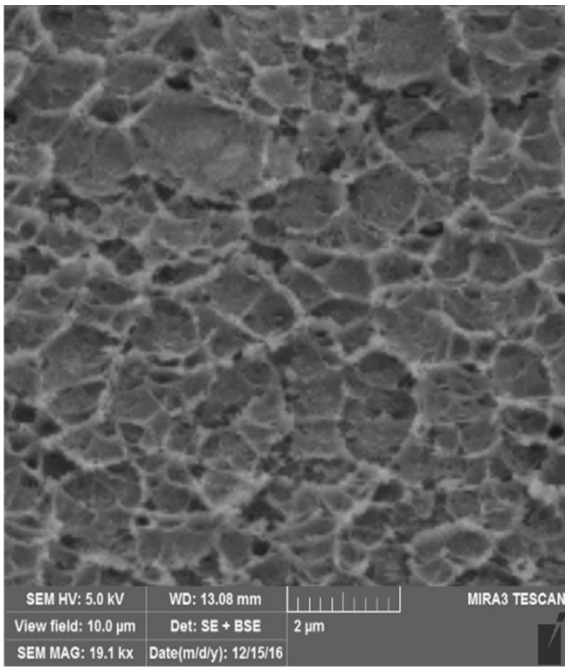

(d) MMM – 10 wt %

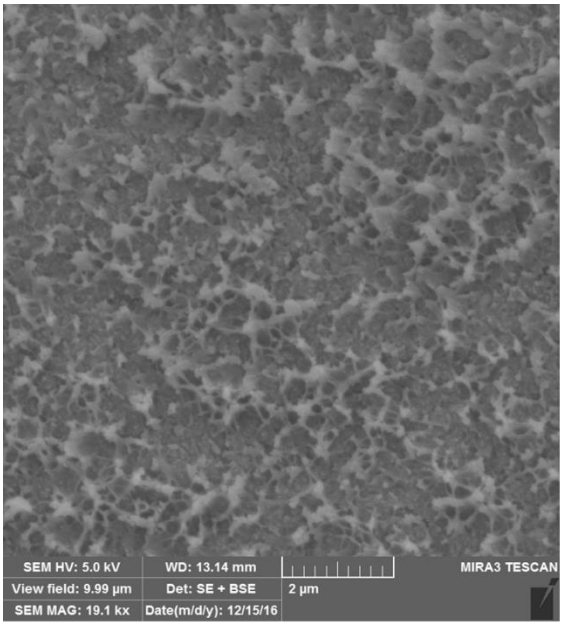

(e) MMM – 20 wt %

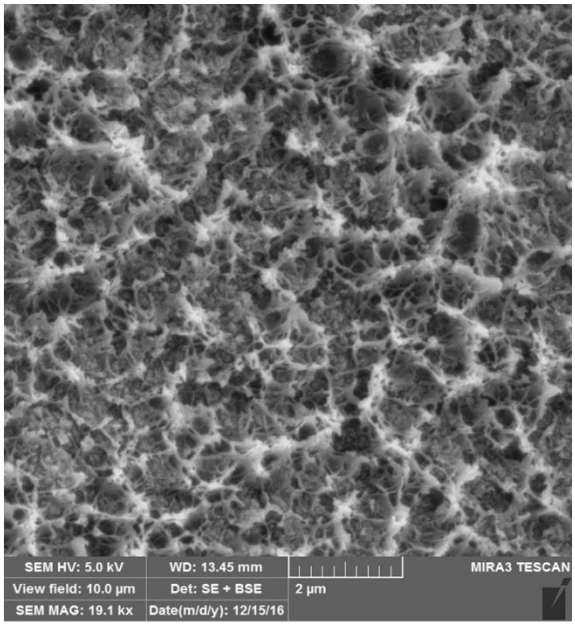

(f) MMM – 30 wt %

Figure 33: SEM images showing Cross-sections of (a) Matrimid and (b) ZIF-8 nanocrystals and (c-f) Cross-sections of MMMs [All membranes annealed at 320°C for 12 h]

To study the crystal structure of the fabricated MMMs and pure Matrimid, their XRD analyses were conducted. XRD results of Matrimid membrane (annealed at 320 °C, 12h), ZIF-8, Mixed Matrix Membrane (5, 10, 20, 30, 40 wt%, annealed at 320°C, 12h) are shown in Fig. 34. Matrimid, being a polymer shows an amorphous broad peak at $2\theta = 17°$ which is in accordance with literature [99]. ZIF-8 shows crystalline structure with peaks at $2\theta = 7.92°$, 13.34° and 18.62°, hence the Mixed Matrix Membranes (5, 10, 20, 30, 40 wt%) which are composed of Matrimid polymer and ZIF-8 filler show peaks with both of their characteristics.

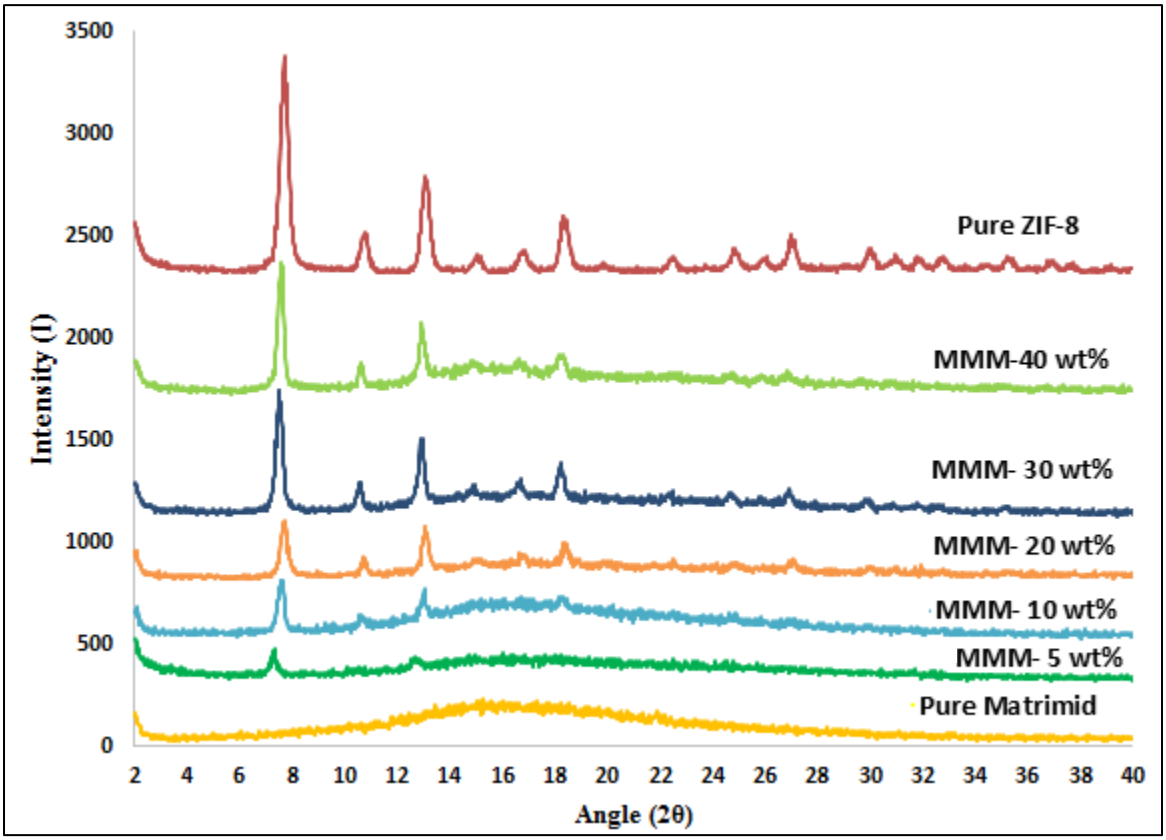

Figure 34: XRD plot of Matrimid, ZIF-8 and MMMs

In order to compare the thermal stabilities of pure Matrimid, ZIF-8 and MMM, their TGA analyses were superimposed in a single graph that shows the wt% versus Temperature.

TGA results of pure Matrimid, ZIF-8 and MMM of Fig. 35 show that MMM (30 wt%, ZIF-8) has intermediate thermal stability between Matrimid and ZIF-8. The weight percentage reduction at 800°C of MMM is 53% while Matrimid and ZIF-8 show 37% and 91% respectively.

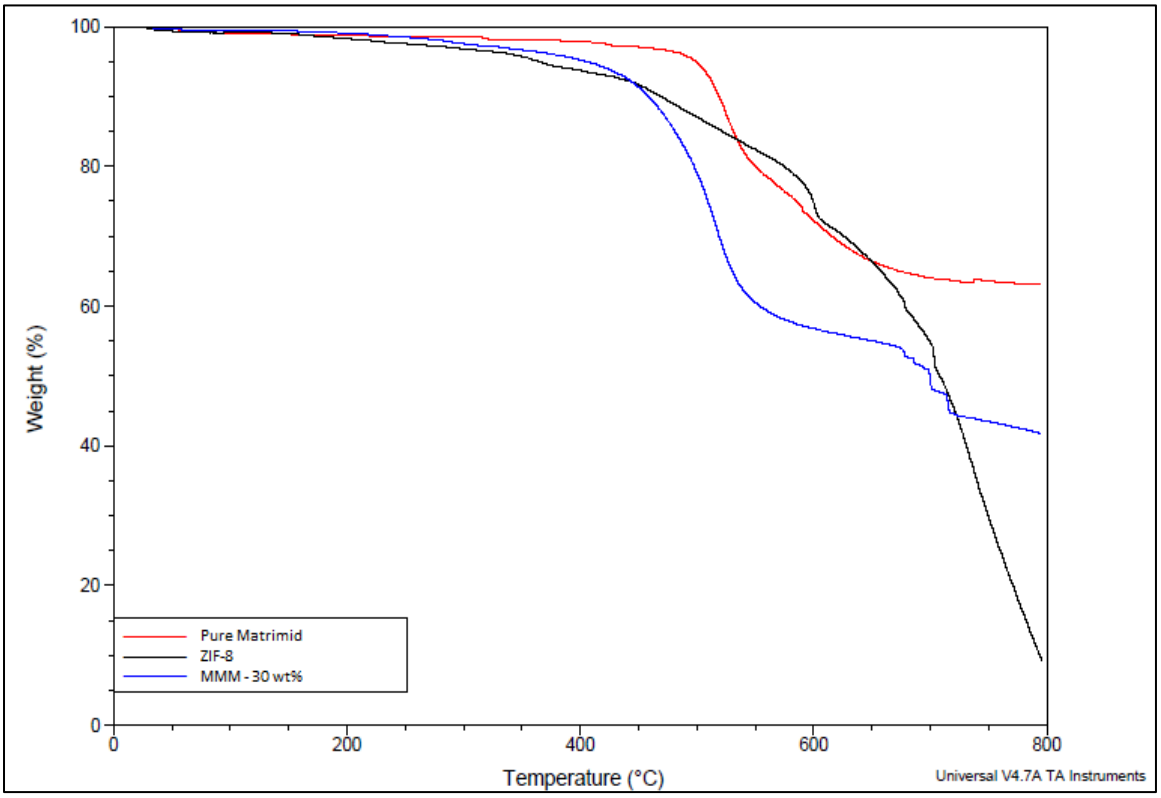

Figure 35: TGA plot of pure Matrimid, ZIF-8 and MMM-30wt%

The effect of loading of ZIF-8 on O_2/N_2 gas separation performance MMMs was studied by conducting single gas permeability test of the annealed MMMs for O_2 and N_2 gases. The feed pressure was 7 bar and the temperature was 23 °C. The results are summarized in the Table 7 and Fig. 36.

Table 7: Permeability test results of various MMMs annealed at 320 °C for 12 hours

Membrane	Permeability (O_2), Barrers	Selectivity (O_2/N_2)	Diffusivity [10^{-8} * cm^2/sec]		Solubility [10^{-3} * cm^3(STP) cm^{-3} $cmHg^{-1}$]	
			O_2	N_2	O_2	N_2
Matrimid	**0.36**	**15.87**	1.36	0.42	2.69	0.55
MMM - 5wt%	**0.33**	**7.40**	1.82	0.51	3.32	1.53
MMM - 10wt%	**0.78**	**8.23**	4.71	0.91	1.66	1.04
MMM - 20wt%	**0.92**	**7.55**	2.34	0.79	3.96	1.56
MMM - 30wt%	**1.24**	**7.90**	3.53	0.66	3.52	2.40
MMM - 40wt%	**1.81**	**7.33**	5.68	1.02	3.19	2.42

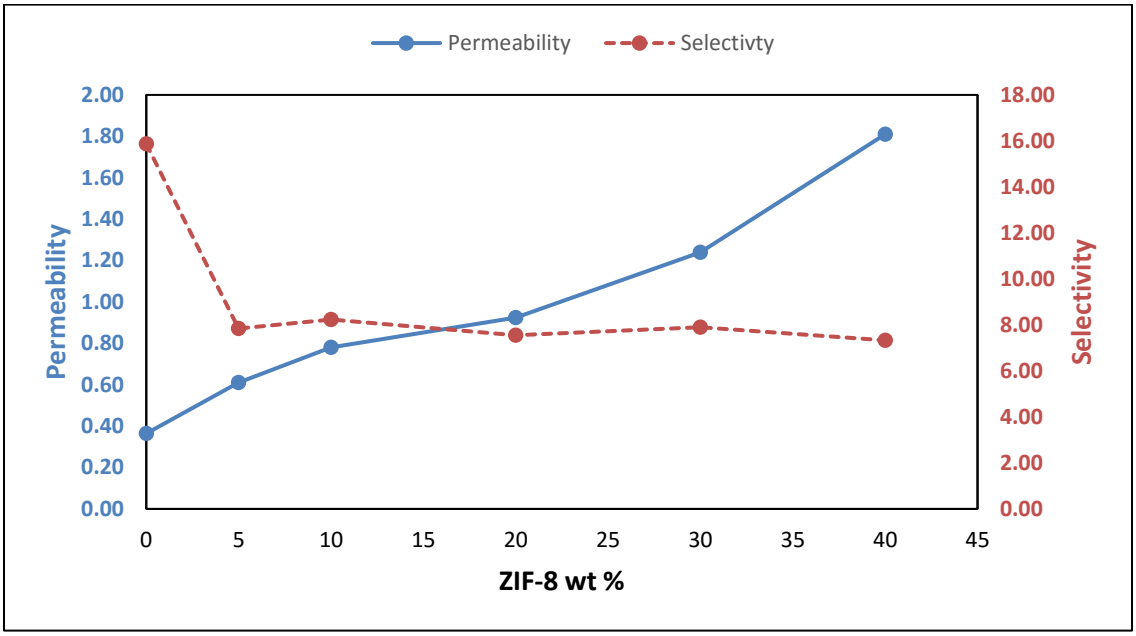

Figure 36: Effect of loading of ZIF-8 on O_2/N_2 gas separation performance of MMMs

It can be observed from the Fig. 36 that permeability of MMMs increased continuously from 0.36 barrers to 1.81 barrers (about 400% increase) as loading of ZIF-8 increased from 0 to 40 wt%. This increase in permeability was expected because ZIF-8 exhibits high permeability and hence the O_2 gas molecules readily permeate through the pores of ZIF-8 cages rather than Matrimid polymer, choosing the least resistance path [25]. Moreover, the introduction of ZIF-8 in Matrimid also results in an increase in the inter polymer chain distance and void formation, thereby creating more free volume for O_2 gas molecules to pass through. It has been reported that introduction of nanoparticles in pure polymer matrix results in disruption of polymer chains thereby increasing the polymer free volume and increased permeability [25]. Therefore, the permeability increment with ZIF-8 loading is due to the combined effect of high permeability of ZIF-8 and the creation of free volume in polymer as a result of introduction of ZIF-8.

The selectivity on the other hand decreased significantly as ZIF-8 was introduced at 5 wt% but as ZIF-8 percentage was increased further, it remained almost the same. Ordonez et.al [25] prepared Matrimid/ZIF8 MMMs and annealed at 240°C. They found that selectivity remains almost the same as the ZIF-8 % was increased from 0-40. However, in the present study there was a sharp decrease in selectivity as ZIF-8 loading was increased from 0-5 wt%. This may be due to the high annealing temperature (320°C), yielding tighter polymer chains. Hence, when ZIF-8 was introduced in Matrimid, macro-voids may have formed resulting in sharp decrease of selectivity.

On one hand, as the amount of ZIF-8 in MMM was increased from 5 to 40 wt%, more free volume is created around the ZIF-8 crystals because more disruption of polymer chain packing takes place due to increased amounts of ZIF-8 [100, 101]. On the other hand, the

increase in loading of ZIF-8 in MMM results in the tighter polymer chain packing thereby reducing free volume in the Matrimid membrane [25, 102]. Thus, these increase and decrease in free volumes may compensate each other and hence the selectivity remained almost the same in MMMs (5 to 40 wt%). The same phenomenon was observed in the works of Song et.al and Ordonez et. al [25, 64].

Another way of visualizing this increase in permeability is by comparing the diffusivity and solubility coefficients. It can be observed that as wt% of ZIF-8 was increased from 0 to 40, the diffusivity of O_2 increased by 3 times while solubility increased slightly. This may be because of the fact the both voids in MMM and increased content of ZIF-8 have contributed to the high diffusivity of O_2 while solubility increased only due to increase of ZIF-8 content in MMM. This also validates the above fact that increase in permeability is due to combination of diffusion of O_2 through ZIF-8 and voids created by introduction of ZIF-8.

The permeability results of MMMs were plotted on Robeson chart of Permeability versus selectivity as shown in Figure 37. The best result was of MMM-40 wt% annealed at 320 °C and 12 hours. Its value was below the Robeson curve due to low selectivity (7.33). Other MMM- 40 wt% membranes were prepared and annealed at 320 °C for longer durations of 18, 24 hours. Their permeabilities were also tested for O_2 and N_2 and were summarized in Table 8. It was found that MMM - 40 wt% (annealed at 320 °C for 24 hours) exhibited permeability of 0.85 barrers and selectivity of 11.79, very close to the Robeson upper bound (2008).

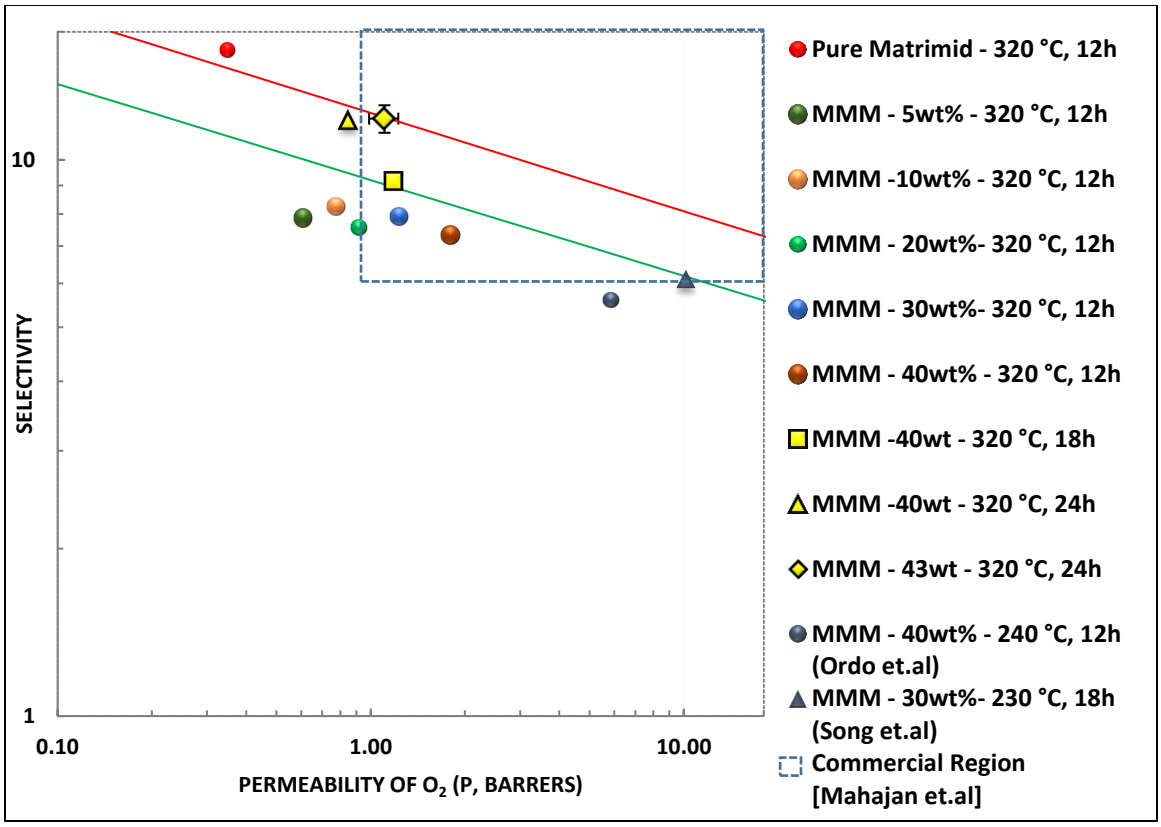

Figure 37: Permeability test results of various MMMs on Robeson plot.

To increase the permeability further, MMM with 43 wt% ZIF-8 was prepared and annealed at 320 °C for 24 hours and its permeability for O_2 and N_2 were also tested and summarized in Table 8. It was found that it had permeability of 1.18 barrers and selectivity of 11.97 which just surpassed the Robeson upper bound (2008) and also located in the commercially attractive region, thus achieving the required objective.

The error analysis was done for the best result of MMM - 43 wt% (320°C, 24 h) and the corresponding error bars are also shown in Fig. 37. Three MMMs were reproduced with 43 wt% ZIF-8 and were annealed at 320°C for 24 h. Then they were tested for permeability of O_2 and N_2 and the average value of permeability was calculated as 1.11 ± 0.12 barrers and selectivity was 11.86 ± 0.68.

This O_2/N_2 gas separation performance is better than the literature work on Matrimid/ZIF8 MMM by Ordonez et.al and Song et.al as their best performances just falls below prior Robeson upper bound [25, 64].

Moreover, Bushell et.al was the only ZIF-8 based Mixed Matrix Membrane which surpassed Robeson present upper bound who used PIM-1 as polymer membrane. In comparison to the PIM-1 which is not commercially available and difficult to fabricate in lab, Matrimid is easily available commercially, hence it stands as an advantage of the present study.

Table 8: Permeability test results of MMMs annealed at 320°C for 18, 24 hrs. (longer durations).

Membrane	Permeability (O_2), Barrers	Selectivity (O_2/N_2)	Diffusivity [10^{-8} * cm^2/sec]		Solubility [10^{-3} * cm^3(STP) cm^{-3} $cmHg^{-1}$]	
			O_2	N_2	O_2	N_2
MMM - 40wt% (320 °C, 18h)	**1.19**	**9.17**	3.26	0.58	3.65	2.23
MMM - 40wt% (320 °C, 24h)	**0.85**	**11.79**	2.38	0.67	3.59	1.09
MMM - 43wt% (320 °C, 24h)	**1.18**	**11.97**	3.95	0.94	2.99	1.05

The effect of chemical treatment on O_2/N_2 gas separation performance of MMMs. was also studied. Ethylene glycol and Ethanol and were selected for chemical treatment because pure Matrimid was known for chemical crosslinking when treated with diols [103], while gas separation performance of Matrimid increased when chemically treated with Ethanol [104]. MMM - 40 wt% (320 °C, 18h) membrane was treated with Ethylene glycol for 1 day and MMM - 40 wt% (320 °C, 12h) membrane with Ethanol for 1 day. The membranes

were then dried at room temperature for 1 day, and the permeability tests for O_2 and N_2 were carried out, and the results were summarized in Table 9.

Table 9: Effect of Chemical treatment on Permeability and Selectivity of MMM

Membrane	Chemical used	Before Chemical Treatment		After Chemical Treatment	
		O_2	O_2/N_2	O_2	O_2/N_2
MMM - 40wt% (320 °C, 18h)	Ethylene Glycol	1.19	9.17	1.12	6.74
MMM - 40wt% (320 °C, 12h)	Ethanol	1.81	7.33	1.44	6.36

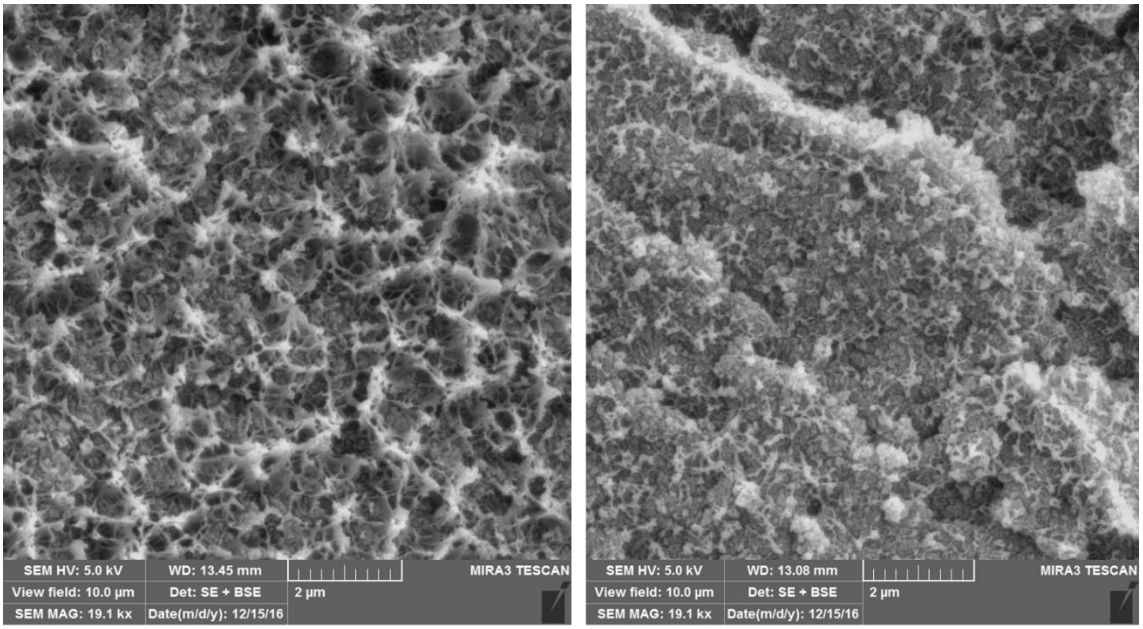

(a) MMM – 30 wt % (b) MMM – 40 wt % (EtOH treated)

Figure 38: SEM Images of (a) MMM-30wt% (b) MMM-40wt% (Ethanol Treated)

The O_2/N_2 gas separation performance of MMMs decreased when chemically treated either with Ethylene Glycol or Ethanol. The chemicals may have crosslinked the Matrimid polymer [103, 104] and filled the voids created by ZIF-8 in polymer chain, which results in the tighter polymer chain packing and smaller free volume. SEM analysis was done post ethanol treatment to find if the voids were crosslinked and filled. The SEM image in Fig. 38 (b) of MMM-40wt% (post ethanol treated) shows less voids compared to MMM-30wt% (Fig. 38(a)).

CHAPTER 5

CONCLUSIONS

In the present study, the effect of annealing temperature and time on O_2/N_2 gas separation performance of Matrimid was studied. The optimum temperature and time was found to be 320°C and 12 h, respectively. Mixed Matrix Membranes were developed by varying the ZIF-8 wt% (5-40%) in Matrimid and annealed at 320°C for 12 h. The effect of ZIF-8 loading on O_2/N_2 gas separation performance of Mixed Matrix Membranes (MMMs) was also studied. All the permeability tests were carried out at a constant feed pressure of 7 bar.

The following conclusions can be drawn from the present work:

- It was found that the selectivity of Matrimid increased significantly with increase in annealing temperature and time. As a result of thermal annealing, rearrangement of the polymer chains occurs resulting in the formation of Charge Transfer Complexes (CTCs). This behavior increases the packing density of the polymer chains and decreases the free volume, thereby increasing selectivity.

- High selectivities of 15.87 and 20.69 for O_2 versus N_2 were achieved by annealing Matrimid at 320°C for 12 and 24 h, respectively. They were found to surpass Robeson present upper bound.

- It was found that as the loading of ZIF-8 in MMM increased (from 5 to 40 wt%), the permeability of MMM increased significantly (from 0.61 to 1.81 barrers, 196% increment) while the selectivity remained almost the same. The permeability

increment with ZIF-8 loading is due to the combined effect of high permeability of ZIF-8 and the creation of free volume in polymer as a result of introduction of ZIF8.

- To enhance the O_2/N_2 gas separation performance further, MMM with 43 wt% ZIF-8 were fabricated and annealed at 320°C for 24 hours which resulted in an average Permeability of 1.11 barrers and Selectivity of 11.86, which surpasses Robeson upper bound and falls into commercially attractive region.

- The effect of chemical treatment on MMMs was also studied by treating MMM-40 wt% membranes with Ethanol and Ethylene Glycol but it resulted in decreased O_2/N_2 gas separation performance in both cases.

SUGGESTED FUTURE RESEARCH

Based on the conducted research in the present study, the following can be recommended for future research:

1) The experimental approach of the present work can be applied to study the annealing effect on other Mixed Matrix Membranes prepared using different set of polymer and filler, so that the overall performance of MMM is improved. For example, Polysulfone has good O_2 permeability of 1.5 barrers and O_2/N_2 selectivity of 5.84 [22] and its selectivity can be enhanced by annealing at higher temperatures and time, thereby optimizing them. Then it can be combined with ZIF-8, which has high permeability to prepare polysulfone/ZIF-8 MMMs and annealed at optimum

temperature and time. Thus MMM with high permeability and selectivity can be prepared, thereby surpassing Robeson curve.

2) All the annealing operations in the present study were done in vacuum environment. Annealing of Mixed Matrix Membranes can be done in other environments such as Helium, Argon etc. to find their effect on gas separation performance.
3) The operating temperature is also an important parameter which effects permeability. In the present study, all permeation experiments were done at room temperature. By varying the operating temperature, activation energy of diffusion changes which effects permeability of gases. Hence, a heating element and temperature controller can be incorporated in permeation cell to study the effect of temperature on permeability and selectivity.
4) All the experiments in the present study were performed using Single Gas permeation set-up. But, considering the practical applications where mixture of gases is used as feed, Mixed Gas permeation experiments can performed.

REFERENCES

[1] R.P. Townsend, Handbook of separation process technology Edited by R. W. Rousseau, Wiley-Interscience, New York, 1987. ISBN 0-471-89558-X, Journal of Chemical Technology & Biotechnology, 44 (1989) 330-331.

[2] T.S. Chung, L.Y. Jiang, Y. Li, S. Kulprathipanja, Mixed matrix membranes (MMMs) comprising organic polymers with dispersed inorganic fillers for gas separation, Progress in Polymer Science (Oxford), 32 (2007) 483-507.

[3] R. Nasir, H. Mukhtar, Z. Man, D.F. Mohshim, Material Advancements in Fabrication of Mixed-Matrix Membranes, Chemical Engineering & Technology, 36 (2013) 717-727.

[4] P. Ball, Scale-up and scale-down of membrane-based separation processes, Membrane Technology, 2000 (2000) 10-13.

[5] Y. Alqaheem, A. Alomair, M. Vinoba, #xe9, A. rez, #xe9, Polymeric Gas-Separation Membranes for Petroleum Refining, International Journal of Polymer Science, 2017 (2017) 19.

[6] S. Alexander Stern, Polymers for gas separations: the next decade, Journal of Membrane Science, 94 (1994) 1-65.

[7] R.W. Spillman, M.B. Sherwin, Gas separation membranes: the first decade, Chemtech, 20 (1990) 378-384.

[8] R.W. Baker, Future Directions of Membrane Gas Separation Technology, Industrial & Engineering Chemistry Research, 41 (2002) 1393-1411.

[9] R.S. Murali, T. Sankarshana, S. Sridhar, Air Separation by Polymer-based Membrane Technology, Separation & Purification Reviews, 42 (2013) 130-186.

[10] S. Majumdar, L.B. Heit, A. Sengupta, K.K. Sirkar, An experimental investigation of oxygen enrichment in a silicone capillary permeator with permeate recycle, Industrial & Engineering Chemistry Research, 26 (1987) 1434-1441.

[11] M. Takht Ravanchi, T. Kaghazchi, A. Kargari, Application of membrane separation processes in petrochemical industry: a review, Desalination, 235 (2009) 199-244.

[12] C. Liu, S. Kulprathipanja, A.M.W. Hillock, S. Husain, W.J. Koros, Recent Progress in Mixed-Matrix Membranes, in: Advanced Membrane Technology and Applications, John Wiley & Sons, Inc., 2008, pp. 787-819.

[13] Y. Yampolskii, Polymeric Gas Separation Membranes, Macromolecules, 45 (2012) 3298-3311.

[14] D. Bastani, N. Esmaeili, M. Asadollahi, Polymeric mixed matrix membranes containing zeolites as a filler for gas separation applications: A review, Journal of Industrial and Engineering Chemistry, 19 (2013) 375-393.

[15] P.S. Goh, A.F. Ismail, S.M. Sanip, B.C. Ng, M. Aziz, Recent advances of inorganic fillers in mixed matrix membrane for gas separation, Separation and Purification Technology, 81 (2011) 243-264.

[16] W.J. Koros, M.R. Coleman, D.R.B. Walker, Controlled Permeability Polymer Membranes, Annual Review of Materials Science, 22 (1992) 47-89.

[17] T.H. Kim, W.J. Koros, G.R. Husk, K.C. O'Brien, Relationship between gas separation properties and chemical structure in a series of aromatic polyimides, Journal of Membrane Science, 37 (1988) 45-62.

[18] J.Y. Park, D.R. Paul, Correlation and prediction of gas permeability in glassy polymer membrane materials via a modified free volume based group contribution method, Journal of Membrane Science, 125 (1997) 23-39.

[19] Y. Xiao, B.T. Low, S.S. Hosseini, T.S. Chung, D.R. Paul, The strategies of molecular architecture and modification of polyimide-based membranes for CO2 removal from natural gas—A review, Progress in Polymer Science, 34 (2009) 561-580.

[20] L.M. Robeson, Polymer membranes for gas separation, Current Opinion in Solid State and Materials Science, 4 (1999) 549-552.

[21] L.M. Robeson, The upper bound revisited, Journal of Membrane Science, 320 (2008) 390-400.

[22] R. Adams, C. Carson, J. Ward, R. Tannenbaum, W. Koros, Metal organic framework mixed matrix membranes for gas separations, Microporous and Mesoporous Materials, 131 (2010) 13-20.

[23] S. Basu, A. Cano-Odena, I.F.J. Vankelecom, MOF-containing mixed-matrix membranes for CO2/CH4 and CO2/N2 binary gas mixture separations, Separation and Purification Technology, 81 (2011) 31-40.

[24] L.Y. Jiang, T.S. Chung, C. Cao, Z. Huang, S. Kulprathipanja, Fundamental understanding of nano-sized zeolite distribution in the formation of the mixed matrix single- and dual-layer asymmetric hollow fiber membranes, Journal of Membrane Science, 252 (2005) 89-100.

[25] M.J.C. Ordoñez, K.J. Balkus Jr, J.P. Ferraris, I.H. Musselman, Molecular sieving realized with ZIF-8/Matrimid® mixed-matrix membranes, Journal of Membrane Science, 361 (2010) 28-37.

[26] E.V. Perez, K.J. Balkus Jr, J.P. Ferraris, I.H. Musselman, Mixed-matrix membranes containing MOF-5 for gas separations, Journal of Membrane Science, 328 (2009) 165-173.

[27] W.A.W. Rafizah, A.F. Ismail, Effect of carbon molecular sieve sizing with poly(vinyl pyrrolidone) K-15 on carbon molecular sieve–polysulfone mixed matrix membrane, Journal of Membrane Science, 307 (2008) 53-61.

[28] J.L.C. Rowsell, O.M. Yaghi, Metal–organic frameworks: a new class of porous materials, Microporous and Mesoporous Materials, 73 (2004) 3-14.

[29] D.Q. Vu, W.J. Koros, S.J. Miller, Mixed matrix membranes using carbon molecular sieves: II. Modeling permeation behavior, Journal of Membrane Science, 211 (2003) 335-348.

[30] C. Zhang, Y. Dai, J.R. Johnson, O. Karvan, W.J. Koros, High performance ZIF-8/6FDA-DAM mixed matrix membrane for propylene/propane separations, Journal of Membrane Science, 389 (2012) 34-42.

[31] Y. Zhang, I.H. Musselman, J.P. Ferraris, K.J. Balkus Jr, Gas permeability properties of Matrimid® membranes containing the metal-organic framework Cu–BPY–HFS, Journal of Membrane Science, 313 (2008) 170-181.

[32] B. Zornoza, C. Tellez, J. Coronas, J. Gascon, F. Kapteijn, Metal organic framework based mixed matrix membranes: An increasingly important field of research with a large application potential, Microporous and Mesoporous Materials, 166 (2013) 67-78.

[33] S.R. Venna, M.A. Carreon, Highly Permeable Zeolite Imidazolate Framework-8 Membranes for CO2/CH4 Separation, Journal of the American Chemical Society, 132 (2010) 76-78.

[34] A. Phan, C.J. Doonan, F.J. Uribe-Romo, C.B. Knobler, M. O'Keeffe, O.M. Yaghi, Synthesis, Structure, and Carbon Dioxide Capture Properties of Zeolitic Imidazolate Frameworks, Accounts of Chemical Research, 43 (2010) 58-67.

[35] K.S. Park, Z. Ni, A.P. Côté, J.Y. Choi, R. Huang, F.J. Uribe-Romo, H.K. Chae, M. O'Keeffe, O.M. Yaghi, Exceptional chemical and thermal stability of zeolitic imidazolate frameworks, Proceedings of the National Academy of Sciences, 103 (2006) 10186-10191.

[36] J. Ahn, W.-J. Chung, I. Pinnau, M.D. Guiver, Polysulfone/silica nanoparticle mixed-matrix membranes for gas separation, Journal of Membrane Science, 314 (2008) 123-133.

[37] M. Moaddeb, W.J. Koros, Gas transport properties of thin polymeric membranes in the presence of silicon dioxide particles, Journal of Membrane Science, 125 (1997) 143-163.

[38] D. Gomes, S.P. Nunes, K.-V. Peinemann, Membranes for gas separation based on poly(1-trimethylsilyl-1-propyne)–silica nanocomposites, Journal of Membrane Science, 246 (2005) 13-25.

[39] M.F.A. Wahab, A.F. Ismail, S.J. Shilton, Studies on gas permeation performance of asymmetric polysulfone hollow fiber mixed matrix membranes using nanosized fumed silica as fillers, Separation and Purification Technology, 86 (2012) 41-48.

[40] Q. Hu, E. Marand, S. Dhingra, D. Fritsch, J. Wen, G. Wilkes, Poly(amide-imide)/TiO2 nano-composite gas separation membranes: Fabrication and characterization, Journal of Membrane Science, 135 (1997) 65-79.

[41] Y. Kong, H. Du, J. Yang, D. Shi, Y. Wang, Y. Zhang, W. Xin, Study on polyimide/TiO2 nanocomposite membranes for gas separation, Desalination, 146 (2002) 49-55.

[42] Y. Xiao, K. Yu Wang, T.-S. Chung, J. Tan, Evolution of nano-particle distribution during the fabrication of mixed matrix -polyimide hollow fiber membranes, Chemical Engineering Science, 61 (2006) 6228-6233.

[43] F. Moghadam, M.R. Omidkhah, E. Vasheghani-Farahani, M.Z. Pedram, F. Dorosti, The effect of TiO2 nanoparticles on gas transport properties of Matrimid5218-based mixed matrix membranes, Separation and Purification Technology, 77 (2011) 128-136.

[44] D. Gomes, I. Buder, S.P. Nunes, Sulfonated silica-based electrolyte nanocomposite membranes, Journal of Polymer Science Part B: Polymer Physics, 44 (2006) 2278-2298.

[45] M.C. Ferrari, M. Galizia, M.G. De Angelis, G.C. Sarti, Gas and Vapor Transport in Mixed Matrix Membranes Based on Amorphous Teflon AF1600 and AF2400 and Fumed Silica, Industrial & Engineering Chemistry Research, 49 (2010) 11920-11935.

[46] A.F. Ismail, L.I.B. David, A review on the latest development of carbon membranes for gas separation, Journal of Membrane Science, 193 (2001) 1-18.

[47] C.M. Zimmerman, A. Singh, W.J. Koros, Tailoring mixed matrix composite membranes for gas separations, Journal of Membrane Science, 137 (1997) 145-154.

[48] M.A. Aroon, A.F. Ismail, T. Matsuura, M.M. Montazer-Rahmati, Performance studies of mixed matrix membranes for gas separation: A review, Separation and Purification Technology, 75 (2010) 229-242.

[49] K.C. Khulbe, C. Feng, T. Matsuura, Synthetic polymeric membranes: characterization by atomic force microscopy, Springer Science & Business Media, 2007.

[50] A. Javaid, Membranes for solubility-based gas separation applications, Chemical Engineering Journal, 112 (2005) 219-226.

[51] M.S. Ray, Diffusion in Zeolites and Other Microporous Solids, by J. Karger and D. M. Ruthven, John Wiley, New York, USA (1992). 605 pages. ISBN 0-47 1-50907-8, Developments in Chemical Engineering and Mineral Processing, 4 (1996) 254-254.

[52] P. Pandey, R.S. Chauhan, Membranes for gas separation, Progress in Polymer Science, 26 (2001) 853-893.

[53] J. Mulder, Basic principles of membrane technology, Springer Science & Business Media, 2012.

[54] S.J. Oh, N. Kim, Y.T. Lee, Preparation and characterization of PVDF/TiO2 organic–inorganic composite membranes for fouling resistance improvement, Journal of Membrane Science, 345 (2009) 13-20.

[55] H. Matsuyama, M. Teramoto, R. Nakatani, T. Maki, Membrane formation via phase separation induced by penetration of nonsolvent from vapor phase. II. Membrane morphology, Journal of Applied Polymer Science, 74 (1999) 171-178.

[56] R.W. Baker, Membrane technology, Wiley Online Library, 2000.

[57] S.V. Sotirchos, V.N. Burganos, Transport of Gases in Porous Membranes, MRS Bulletin, 24 (2013) 41-45.

[58] W.J. Koros, G.K. Fleming, Membrane-based gas separation, Journal of Membrane Science, 83 (1993) 1-80.

[59] J.G. Wijmans, R.W. Baker, The solution-diffusion model: a review, Journal of Membrane Science, 107 (1995) 1-21.

[60] R. Mahajan, R. Burns, M. Schaeffer, W.J. Koros, Challenges in forming successful mixed matrix membranes with rigid polymeric materials, Journal of Applied Polymer Science, 86 (2002) 881-890.

[61] Ş.B. Tantekin-Ersolmaz, Ç. Atalay-Oral, M. Tatlıer, A. Erdem-Şenatalar, B. Schoeman, J. Sterte, Effect of zeolite particle size on the performance of polymer–zeolite mixed matrix membranes, Journal of Membrane Science, 175 (2000) 285-288.

[62] R. Mahajan, W.J. Koros, Factors Controlling Successful Formation of Mixed-Matrix Gas Separation Materials, Industrial & Engineering Chemistry Research, 39 (2000) 2692-2696.

[63] J.N. Barsema, S.D. Klijnstra, J.H. Balster, N.F.A. van der Vegt, G.H. Koops, M. Wessling, Intermediate polymer to carbon gas separation membranes based on Matrimid PI, Journal of Membrane Science, 238 (2004) 93-102.

[64] Q. Song, S.K. Nataraj, M.V. Roussenova, J.C. Tan, D.J. Hughes, W. Li, P. Bourgoin, M.A. Alam, A.K. Cheetham, S.A. Al-Muhtaseb, E. Sivaniah, Zeolitic imidazolate framework (ZIF-8) based polymer nanocomposite membranes for gas separation, Energy & Environmental Science, 5 (2012) 8359-8369.

[65] A. Bos, I.G.M. Pünt, M. Wessling, H. Strathmann, Plasticization-resistant glassy polyimide membranes for CO2/CO4 separations, Separation and Purification Technology, 14 (1998) 27-39.

[66] J. Ahmad, M.-B. Hägg, Development of matrimid/zeolite 4A mixed matrix membranes using low boiling point solvent, Separation and Purification Technology, 115 (2013) 190-197.

[67] H.H. Yong, H.C. Park, Y.S. Kang, J. Won, W.N. Kim, Zeolite-filled polyimide membrane containing 2,4,6-triaminopyrimidine, Journal of Membrane Science, 188 (2001) 151-163.

[68] P.S. Tin, T.S. Chung, Y. Liu, R. Wang, S.L. Liu, K.P. Pramoda, Effects of cross-linking modification on gas separation performance of Matrimid membranes, Journal of Membrane Science, 225 (2003) 77-90.

[69] L. Shao, L. Liu, S.-X. Cheng, Y.-D. Huang, J. Ma, Comparison of diamino cross-linking in different polyimide solutions and membranes by precipitation observation and gas transport, Journal of Membrane Science, 312 (2008) 174-185.

[70] B. Wang, A.P. Cote, H. Furukawa, M. O/'Keeffe, O.M. Yaghi, Colossal cages in zeolitic imidazolate frameworks as selective carbon dioxide reservoirs, Nature, 453 (2008) 207-211.

[71] H.-L. Jiang, B. Liu, T. Akita, M. Haruta, H. Sakurai, Q. Xu, Au@ZIF-8: CO Oxidation over Gold Nanoparticles Deposited to Metal−Organic Framework, Journal of the American Chemical Society, 131 (2009) 11302-11303.

[72] G. Lu, J.T. Hupp, Metal−Organic Frameworks as Sensors: A ZIF-8 Based Fabry−Pérot Device as a Selective Sensor for Chemical Vapors and Gases, Journal of the American Chemical Society, 132 (2010) 7832-7833.

[73] X.-C. Huang, Y.-Y. Lin, J.-P. Zhang, X.-M. Chen, Ligand-Directed Strategy for Zeolite-Type Metal–Organic Frameworks: Zinc(II) Imidazolates with Unusual Zeolitic Topologies, Angewandte Chemie, 118 (2006) 1587-1589.

[74] Y. Pan, Y. Liu, G. Zeng, L. Zhao, Z. Lai, Rapid synthesis of zeolitic imidazolate framework-8 (ZIF-8) nanocrystals in an aqueous system, Chemical Communications, 47 (2011) 2071-2073.

[75] J. Cravillon, R. Nayuk, S. Springer, A. Feldhoff, K. Huber, M. Wiebcke, Controlling Zeolitic Imidazolate Framework Nano- and Microcrystal Formation: Insight into Crystal Growth by Time-Resolved In Situ Static Light Scattering, Chemistry of Materials, 23 (2011) 2130-2141.

[76] S.R. Venna, J.B. Jasinski, M.A. Carreon, Structural Evolution of Zeolitic Imidazolate Framework-8, Journal of the American Chemical Society, 132 (2010) 18030-18033.

[77] L. Diestel, X.L. Liu, Y.S. Li, W.S. Yang, J. Caro, Comparative permeation studies on three supported membranes: Pure ZIF-8, pure polymethylphenylsiloxane, and mixed matrix membranes, Microporous and Mesoporous Materials, 189 (2014) 210-215.

[78] A.F. Bushell, M.P. Attfield, C.R. Mason, P.M. Budd, Y. Yampolskii, L. Starannikova, A. Rebrov, F. Bazzarelli, P. Bernardo, J. Carolus Jansen, M. Lanč, K. Friess, V. Shantarovich, V. Gustov, V. Isaeva, Gas permeation parameters of mixed matrix membranes based on the polymer of intrinsic microporosity PIM-1 and the zeolitic imidazolate framework ZIF-8, Journal of Membrane Science, 427 (2013) 48-62.

[79] K. Díaz, M. López-González, L.F. del Castillo, E. Riande, Effect of zeolitic imidazolate frameworks on the gas transport performance of ZIF8-poly(1,4-phenylene ether-ether-sulfone) hybrid membranes, Journal of Membrane Science, 383 (2011) 206-213.

[80] B. Zornoza, B. Seoane, J.M. Zamaro, C. Téllez, J. Coronas, Combination of MOFs and Zeolites for Mixed-Matrix Membranes, ChemPhysChem, 12 (2011) 2781-2785.

[81] S.N. Wijenayake, N.P. Panapitiya, S.H. Versteeg, C.N. Nguyen, S. Goel, K.J. Balkus, I.H. Musselman, J.P. Ferraris, Surface Cross-Linking of ZIF-8/Polyimide Mixed Matrix Membranes (MMMs) for Gas Separation, Industrial & Engineering Chemistry Research, 52 (2013) 6991-7001.

[82] H. Vinh-Thang, S. Kaliaguine, Predictive Models for Mixed-Matrix Membrane Performance: A Review, Chemical Reviews, 113 (2013) 4980-5028.

[83] Z. Huang, Y. Li, R. Wen, M. May Teoh, S. Kulprathipanja, Enhanced gas separation properties by using nanostructured PES-Zeolite 4A mixed matrix membranes, Journal of Applied Polymer Science, 101 (2006) 3800-3805.

[84] Y. Dai, J.R. Johnson, O. Karvan, D.S. Sholl, W.J. Koros, Ultem®/ZIF-8 mixed matrix hollow fiber membranes for CO2/N2 separations, Journal of Membrane Science, 401–402 (2012) 76-82.

[85] C. Özgen, Production and performance evaluation of ZIF-8 based binary and ternary mixed matrix gas separation membranes, in, MIDDLE EAST TECHNICAL UNIVERSITY, 2012.

[86] J. Dechnik, J. Gascon, C. Doonan, C. Janiak, C.J. Sumby, New directions for mixed-matrix membranes, Angewandte Chemie International Edition, (2017) n/a-n/a.

[87] T.-H. Bae, J.S. Lee, W. Qiu, W.J. Koros, C.W. Jones, S. Nair, A High-Performance Gas-Separation Membrane Containing Submicrometer-Sized Metal–Organic Framework Crystals, Angewandte Chemie International Edition, 49 (2010) 9863-9866.

[88] M.G. Süer, N. Baç, L. Yilmaz, Gas permeation characteristics of polymer-zeolite mixed matrix membranes, Journal of Membrane Science, 91 (1994) 77-86.

[89] B.A. Al-Maythalony, A.M. Alloush, M. Faizan, H. Dafallah, M.A.A. Elgzoly, A.A.A. Seliman, A. Al-Ahmed, Z.H. Yamani, M.A.M. Habib, K.E. Cordova, O.M. Yaghi, Tuning the Interplay between Selectivity and Permeability of ZIF-7 Mixed Matrix Membranes, ACS Applied Materials & Interfaces, (2017).

[90] P.M. Budd, N.B. McKeown, Highly permeable polymers for gas separation membranes, Polymer Chemistry, 1 (2010) 63-68.

[91] L. Ansaloni, M. Minelli, M. Giacinti Baschetti, G.C. Sarti, Effects of Thermal Treatment and Physical Aging on the Gas Transport Properties in Matrimid®, Oil Gas Sci. Technol. – Rev. IFP Energies nouvelles, 70 (2015) 367-379.

[92] O.G. Nik, X.Y. Chen, S. Kaliaguine, Amine-functionalized zeolite FAU/EMT-polyimide mixed matrix membranes for CO2/CH4 separation, Journal of Membrane Science, 379 (2011) 468-478.

[93] O.G. Nik, X.Y. Chen, S. Kaliaguine, Functionalized metal organic framework-polyimide mixed matrix membranes for CO_2/CH_4 separation, Journal of Membrane Science, 413–414 (2012) 48-61.

[94] J.J. Krol, M. Boerrigter, G.H. Koops, Polyimide hollow fiber gas separation membranes: Preparation and the suppression of plasticization in propane/propylene environments, Journal of Membrane Science, 184 (2001) 275-286.

[95] H. Kawakami, M. Mikawa, S. Nagaoka, Gas transport properties in thermally cured aromatic polyimide membranes, Journal of Membrane Science, 118 (1996) 223-230.

[96] F.J. Dinan, W.T. Schwartz, R.A. Wolfe, D.S. Hojnicki, T.S. Clair, J.R. Pratt, Solid-State 13C-NMR spectral evidence for charge transfer complex formation in aromatic diimides and dianhydrides, Journal of Polymer Science Part A: Polymer Chemistry, 30 (1992) 111-118.

[97] M. Hasegawa, K. Horie, Photophysics, photochemistry, and optical properties of polyimides, Progress in Polymer Science, 26 (2001) 259-335.

[98] S.M. Davoodi, M. Sadeghi, M. Naghsh, A. Moheb, Olefin-paraffin separation performance of polyimide Matrimid[registered sign]/silica nanocomposite membranes, RSC Advances, 6 (2016) 23746-23759.

[99] M. Peydayesh, S. Asarehpour, T. Mohammadi, O. Bakhtiari, Preparation and characterization of SAPO-34 – Matrimid® 5218 mixed matrix membranes for CO2/CH4 separation, Chemical Engineering Research and Design, 91 (2013) 1335-1342.

[100] W. Yave, S. Shishatskiy, V. Abetz, S. Matson, E. Litvinova, V. Khotimskiy, K.-V. Peinemann, A Novel Poly(4-methyl-2-pentyne)/TiO2 Hybrid Nanocomposite Membrane for Natural Gas Conditioning: Butane/Methane Separation, Macromolecular Chemistry and Physics, 208 (2007) 2412-2418.

[101] T.C. Merkel, B.D. Freeman, R.J. Spontak, Z. He, I. Pinnau, P. Meakin, A.J. Hill, Ultrapermeable, Reverse-Selective Nanocomposite Membranes, Science, 296 (2002) 519-522.

[102] M.G. Süer, N. Baç, L. Yilmaz, Gas permeation characteristics of polymer-zeolite mixed matrix membranes, Journal of Membrane Science, 91 (1994) 77-86.

[103] K. Vanherck, G. Koeckelberghs, I.F. Vankelecom, Crosslinking polyimides for membrane applications: a review, Progress in polymer science, 38 (2013) 874-896.

[104] P.S. Tin, T.-S. Chung, A.J. Hill, Advanced fabrication of carbon molecular sieve membranes by nonsolvent pretreatment of precursor polymers, Industrial & engineering chemistry research, 43 (2004) 6476-6483.

APPENDIX

CALCULATION OF %YIELD OF ZIF-8

Zinc Nitrate Hexahydrate [$Zn(NO_3)_2.6H_2O$], 2-methylimidazole [2- MeIm] and Methanol [CH_3OH] were mixed in the molar ratio of 1 : 4 : 1500 for the synthesis of ZIF-8 by the method described in Chap. 3. The final product was **0.129 g** of ZIF-8 (Practical yield)

$$\%\,\boldsymbol{Yield} = \frac{\boldsymbol{Pratical\ yield\ (from\ experiment)}}{\boldsymbol{Theoretical\ yield\ (from\ chemical\ reaction)}}$$

Materials used and their Molar ratio calculation:

S.No.	Chemical	Formula	Mol.wt (g/mole)	Mass (g)	Moles	Molar Ratio Zn^{+2}:MeIm: Me
1	Zinc Nitrate	$Zn(NO_3)_2.6H_2O$	297.49	0.7344	0.002469	1 : 4 : 1500
2	2-Methyl imidazole	$C_4H_6N_2$	82.104	0.8106	0.009873	
3	Methanol	CH_3OH	32.04	118.65	3.703184	
4	ZIF-8	$Zn_6N_{24}C_{48}H_{60}$	1365.51	0.129		

The chemical reaction involved in the synthesis of ZIF-8 is

$$6\,Zn(NO_3)_2.6H_2O + 12\,C_4H_6N_2 + CH_3OH \rightarrow Zn_6N_{24}C_{48}H_{60}$$

6 moles of Zinc Nitrate + 12 moles of 2-MeIm + 1 mole of Methanol --> 1 mole of ZIF-8

6 moles of Zinc nitrate → 1 mole of ZIF-8

6*(297.49) g of Zinc Nitrate → 1365.51 g of ZIF-8

0.7344 g of Zinc Nitrate → 0.5612 g of ZIF-8

Therefore, Theoretical yield of ZIF-8 is **0.5612 g**

$$\%\,\boldsymbol{Yield} = \frac{\boldsymbol{Pratical\ yield\ (from\ experiment)}}{\boldsymbol{Theoretical\ yield\ (from\ chemical\ reaction)}} = \frac{0.129\ g}{0.561\ g}$$

$$= \mathbf{22.9}\ \%$$

VITAE

Name : Ameruddin Mohammed Khaja

Nationality : India

Date of Birth : 07/09/1991

Email : mkameruddin@gmail.com

Permanent Address : Hyderabad, India

Academic Background : **M.S in Materials Science Engineering,**

King Fahd University of Petroleum & Minerals,

Kingdom of Saudi Arabia [May, 2017]

B.Tech in Metallurgical and Materials Science Engg.,

NIT Warangal,

India [April, 2013]